Accepted Manuscript

Please cite this article as: Costa-Trigo, I., Otero-Penedo, P., Outeiriño, D., Paz, A., & Domínguez, J. M. (2019). Valorization of chestnut (castanea sativa) residues: Characterization of different materials and optimization of the acid-hydrolysis of chestnut burrs for the elaboration of culture broths. *Waste Management*, 87, 472-484. doi:10.1016/j.wasman.2019.02.028

Link to published version: https://doi.org/10.1016/j.wasman.2019.02.028

Valorization of chestnut (*Castanea sativa*) residues: characterization of different materials and optimization of the acid-hydrolysis of chestnut burrs for the elaboration of culture broths

Abstract

Four kinds of waste from the industrial processing of chestnuts (*Castanea sativa*), namely leaves, pruned material and burrs from chestnut tree plus chestnut shells, were characterized to determine their content in polymers and thus their potential use in biorefinery processes. Results revealed that chestnut burrs have the highest polysaccharide content being the most promising for carrying out the subsequent stages of acid hydrolysis. Treatment with diluted sulfuric acid (prehydrolysis) allowed the solubilization of xylose, glucose and arabinose, but also some toxic compounds such as furan derivatives, aliphatic acids and phenolic constituents. Xylose, the main component released in the hemicellulosic hydrolyzates, was maximized by using a 3**(2-0) full factorial design combined with desirability function. At optimum conditions set at 130ºC and 3% (w/v) H_2SO_4, this value was 22.6 g L^{-1} xylose. Three concentrations of activated charcoal (1, 2.5 and 5% w/v) were evaluated to remove certain unwanted byproducts, and it was found that under the highest dosage, 95.27±0.03% of the color was removed with an almost total reduction of furan derivatives, making this liquor an appropriate basis for the development of suitable culture media for lactic acid bacteria. To validate this hypothesis three lactic acid bacteria, namely *Lactobacillus plantarum, Lactobacillus pentosus* and *Lactococcus lactis* were positively tested finding lactic acid yields of 0.89, 0.92 and 0.83 g/L·h respectively.

Keywords: chestnut wastes, prehydrolysis, hemicellulosic hydrolyzates, activated charcoal, detoxification.

1. Introduction

A current concern in Europe's agro-food sector is the search for a productive use of the thousands of tons of crop wastes generated yearly, given that such waste involves significant economic and environmental management costs (Aires et al., 2016). For instance, in 2016 the Mediterranean countries alone produced and processed about 143,256 tons of chestnuts (*Castanea sativa*), the main European producers being Italy (36%), Greece (22%), Portugal (19%) and Spain (11%) ("FAOSTAT," 2018). In the region of Galicia (NW of Spain), the food industry uses about 7,000 tons per year of chestnuts for the production of marron-glacé, chestnut purée and other products (Santos et al., 2017). This industry generates tons of waste, including leaves, prunings and burrs from chestnut trees as well as chesnut shells.

These residues have typically been left in the soil, promoting the growth of insect larvae and consequently leading to crop damage (Vázquez et al., 2012), or they are burned in the field, impacting negatively on the atmosphere and the land, and representing one of the main sources of toxic emissions (some of these similar to dioxins, e.g., CO, NOx, long-chain/aromatic hydrocarbons, polychlorodibenzodioxins) (Morana et al. 2017) and pollutants, if pesticides and heavy metals remain in the composition of the ash (Picchi et al. 2018). Currently, new strategies such as composting are being considered (Ventorino et al. 2016). However, on the same lines as the refining of petroleum, which produces multiple fuels and chemicals, the concept of biorefinery establishes that lignocellulosic biomass can be fractionated into its three main compounds (cellulose, hemicelluloses and lignin) that can then be further converted into a variety of high volume liquid fuels and high value chemicals (Smichi et al. 2018). Therefore, the cell walls of lignocellulosic materials can be degraded into their constituents by hydrolytic processes (acid-catalyzed or hydrothermals), turning them into mixtures of oligomeric and monomeric sugars such as xylose, mannose,

galactose, arabinose, hydroxycinnamic and acetic acids from the non-cellulose polysaccharides. That is, lignocellulosic biomass is a source of compounds that can be transformed into high value-added products such as bio oil, biogas, or other bio-based chemicals with a wide array of industrial applications (Arevalo-Gallegos et al. 2017; Bhowmick et al. 2018). During the optimization of the hemicellulosic hydrolysis, the objective is to obtain the highest yield of sugars, but also to minimize the formation of compounds which can be inhibitory of microbial growth, by adjusting parameters such as temperature, acid concentration, liquid-to-solid ratio and reaction time (Brito et al., 2018).

Although the tolerance to inhibitory compounds depends on the microorganism used and the operational conditions assayed, a reduction in the concentration of microbial inhibitors might decrease fermentation times and increase the efficiency of sugar use and product formation (Mateo et al., 2013). Detoxification with activated charcoal has been widely reported to remove those phenolic compounds (among others) present in acid hydrolyzates obtained from different materials including chestnut (*Castanea sativa*) shells (Morana et al., 2017), palm press fiber (Brito et al., 2018), potato peels, wheat bran, barley bran (Karasu-yalcin, 2016), olive tree pruning residue (Mateo et al., 2013) and corncob (Gupta et al., 2017).

Raw or detoxified hemicellulosic hydrolyzates have been assayed as culture media for several applications, including the production of lactic acid (Alves de Oliveira et al., 2019), bacteriocins (Paz et al. 2017), biosurfactants (Brito et al., 2018), biogas (Santos et al. 2018) and xylitol (Bustos Vázquez et al. 2017), among others. Although many microorganisms have been employed, the use of lactic acid bacteria (LAB) have a high potential because they are safe for human consumption and because they produce various antimicrobial compounds such as organic acids, including lactic acid (da Silva Sabo et al., 2017). Therefore, lactic acid obtained by fermentative processes finds applications not only in the

food industry but also in the chemical, cosmetic, and pharmaceutical sectors, as well as a great potential for the production of biodegradable and biocompatible polylactic polymers that can be employed from packaging to fibers and foams (Portilla Rivera et al., 2015). However, LAB are catalogued as fastidious-growing microorganisms with numerous requirements for growth including amino acids, peptides, vitamins, and nucleic acids (Rodríguez-Pazo et al., 2016).

Chestnut wastes are a source of carbohydrates susceptible to be used in biorefineries. The current study deals with the characterization of four kinds of waste from the industrial processing of chestnuts (*Castanea sativa*), and the subsequent selection of the material with the highest polysaccharide content. Chestnut burrs were fractionated by acid-prehydrolysis and the process optimized through an incomplete factorial design to maximize the amount of xylose released. Finally, in order to formulate suitable culture media, the hemicellulosic hydrolyzates were neutralized and detoxified with charcoal to reduce color and the concentration of inhibitory compounds. The suitability of this culture medium was validated with three lactic acid bacteria: *Lactococcus lactis* subsp. *lactis* CECT 4434, *Lactobacillus pentosus* CECT 4023 and *Lactobacillus plantarum* CECT 221, selected due to their high nutritional requirements.

2. Material and methods

2.1. Chemicals

All chemicals and reagents used in this study were of analytical grade and obtained from Panreac Química SLU (Barcelona, Spain) and Sigma–Aldrich (St. Louis, MO, USA). The solvents employed were of high-performance liquid chromatography (HPLC) grade, and water was ultra-pure. HPLC calibration curves were created for all the standards by injection of different stock concentrations.

2.2. Materials

The study uses four residues obtained from the harvesting and processing of chestnuts, namely leaves, prunings and burrs of the chestnut tree and chestnut shells. All these materials were obtained from local cultivars harvested in September/October 2016 in Galicia, north-west Spain, and supplied by Soutos Sativa S.L., (Monterroso, Lugo, Spain), a local company involved in the cultivation, processing and commercialization of chestnuts. The samples were dried at room temperature before submitting them to grinding, sieving and homogenization to obtain a homogenous material, prior to the storage and conservation at room temperature so as to guarantee stability until use.

2.3. Microorganism and culture media

Lactococcus lactis subsp. *lactis* CECT 4434, *Lactobacillus pentosus* CECT 4023 and *Lactobacillus plantarum* CECT 221 were obtained from the Spanish Collection of Type Cultures (Valencia, Spain) and maintained in cryovials on 30% (v/v) glycerol and growth media at -80 ºC. The strains were grown for 24h on plates using the Man-Rogosa-Sharpe (MRS) medium formulated with 10 g L^{-1} peptone, 8 g L^{-1} beef extract, 4 g L^{-1} yeast extract, 20 g L^{-1} D-glucose, 2 g L^{-1} K_2HPO_4, 2 g L^{-1} di-ammonium hydrogen citrate, 5 g L^{-1} CH_3COONa, 0.2 g L^{-1} $MgSO_4 \cdot 7H_2O$, 0.05 g L^{-1} $MnSO_4 \cdot 2H_2O$, 1 g L^{-1} Tween-80 and 20 g L^{-1} agar. A loop full of a slant culture was transferred to 250 mL Erlenmeyer flasks containing 100 mL of MRS medium without agar and incubated for 24h at 30 ºC and 150 rpm in orbital shaker (Optic Ivymen System, Comecta S.A., distributed by Scharlab, Madrid, Spain).

Cells were recovered by centrifugation (Ortoalresa, Consul 21, EBA 20, Hettich Zentrifugen, Germany) at 3700 × *g* for 15 min and rinsed twice with sterile phosphate buffer saline (PBS) at pH 7.4 (containing 10 mM KH_2PO_4 $K_2HPO_4^{-1}$ and 150 mM NaCl) before inoculation (Bustos et al., 2018).

2.4. Characterization of plant materials

Plant materials were oven-dried (Binder-Model 53 ED, Tuttlingen, Germany) to a constant weight at 105ºC in order to determine the percentage of humidity. The ash content was measured using a muffle furnace (Carbolite ELF 11/6B with 301 controller, Derbyshire, United Kingdom) for 6 h at 575ºC. Nitrogen and carbon percentages were analyzed using a Thermo Finningan Flash Elemental Analyzer 1112 series, San Jose, CA (USA). The composition of plant materials was determined by quantitative acid hydrolysis in two-stages (Paz et al., 2018). Briefly, each material was treated for 1h with 72 wt% sulfuric acid at 30ºC, then sulfuric acid was diluted to 4 wt% and heated at 121ºC for 1 h. The solid residue obtained after hydrolysis was oven-dried at 105ºC and considered as Klason lignin. The analysis of the liquid fraction by High Performance Liquid Chromatography (HPLC) is described below. The quantitative acid hydrolysis liquor was diluted 10 times with 4 wt% sulfuric acid and measured at an absorbance of 205 nm in a UV-Vis Spectrophotometer (Libra S60-Biochrom, Cambridge, U.K.) to determine the acid-soluble lignin. The contents of the extracts were obtained after leaving the material (1-5 g) under reflux for 12-24 hours using ethanol (Ethanol absolute, reagent grade, ACS, ISO, Scharlau, Sentmenat, Barcelona, Spain) as a solvent in a Soxhlet (Behrotest In-Line Extraction Units, Behr Labor-Technik, distributed by Fisher Scientific, Madrid, Spain).

The minerals K, Cu, Fe, Mn, Mg, Ca, Na, Si and Zn were measured in an Atomic Absorption Spectrometer Varian SpectrAA 220 Fast Sequential (Varian Inc., Palo Alto, CA, USA). The metallic elements Cr, Ni, Pb, and Al were determined using an ICP-MS Thermo Elemental X7 (Waltham, Massachusetts, USA). All mineral elements were quantified after acid digestion using 0.4 g of the sample with 8 mL HNO_3 and 3 mL H_2O_2 in a Microwave (CEM, MARSXpress model, Matthews, North Carolina, USA).

All parameters were performed in triplicate and standard deviations reported.

151 **2.5. Hydrolytic treatments**

152 Lignocellulosic material was hydrolyzed with diluted sulfuric acid (prehydrolysis) in an
153 autoclave (Trade Raypa SL, Terrassa, Barcelona) using a liquid/solid ratio of 8 g/g.
154 Aliquots from the reaction media were taken, cooled, filtered with 0.45 μm membranes
155 and analyzed by HPLC using the procedure described below. The effect of time was
156 evaluated with dried chestnut burrs using 3% (w/v) H_2SO_4 and 130°C for 15, 30 and 60
157 min in 250 mL Pyrex bottles. Hydrolyses were carried out in triplicate and mean values
158 and their standard deviations reported in the corresponding Tables.

159 **2.6. Box–Behnken response surface methodology**

160 A 3**(2-0) full factorial design was planned to optimize the release of carbohydrates using
161 the hydrolysis time previously optimized (30 min). The design contained two independent
162 variables at three levels (−1, 0, 1). The values of these independent variables were:
163 temperature (100, 115, and 130ºC) and H_2SO_4 concentration (1, 3, and 5% w/v). For
164 statistical calculations, the independent variables were coded as x_1 and x_2, respectively,
165 according to the equations:

166 $$x_1 = (T - 115)/15 \quad \text{(Eq. 1)}$$

167 and

168 $$x_2 = ([H_2SO_4] - 3)/2 \quad \text{(Eq. 2)}$$

169 The dependent variables studied were the concentration of the main components released
170 (g L^{-1}): glucose (y_1), xylose (y_2), arabinose (y_3), acetic acid (y_4), furfural (y_5) and 5-
171 hydroxymethylfurfural (HMF) (y_6).

172 The design was carried out in one block comprising 12 experimental runs including 9
173 factorial experiments, and three additional replicates at the center of the experimental
174 domain (0) for the estimation of the pure error. This type of designs allows for the
175 estimation of the significance of the individual parameters and their interactions.

The influence of the independent variables on the dependent variables was assessed using the Statistic software package version 8.0 (Stat Soft, USA). The responses obtained were subjected to analysis of variance (ANOVA). The statistical significance of the independent variables on the responses was determined by evaluating the probability *p*-value and Fisher's test with a 95% confidence level obtained from the ANOVA. Data from the factorial design were subjected to a second-order multiple regression analysis using a least squares regression methodology to obtain parameters of the mathematical model. The interrelationship between dependent variable y_i and operational variables was fitted by a polynomial quadratic equation established through a model including linear, quadratic and interaction terms:

$$y_i = b_0 + b_1x_1 + b_{11}x_1^2 + b_2x_2 + b_{22}x_2^2 + b_{12}x_1x_2 \quad \text{(Eq. 3)}$$

where y_i is the predicted response; x_1 and x_2 are the coded independent variables; b_0 is the model constant; b_1 and b_2 are linear coefficients; b_{11} and b_{22} are quadratic coefficients; and b_{12} are the lineal cross-product coefficients. For each run, predicted values were calculated from the regression equation.

The quality of the polynomial model equation was expressed by determining coefficient R^2, adjusted R^2, and lack of fit. Tridimensional surface plots illustrate the relationship and interaction between coded variables and the responses.

2.7. Optimization of the operational conditions and validation of the model

The profile for predicted values and desirability option from the Statistic software package version 8.0 (Stat Soft, USA) was used for the optimization of the xylose released, as well as for validation of the experimental model.

198 **2.8. Neutralization and detoxification of hemicellulosic hydrolyzates and fermentation**
199 **conditions**
200 The liquid phase from the acid hydrolysis was neutralized with NaOH to a final pH of 7.0
201 (Seong et al., 2016). Neutralized hydrolyzates were detoxified with activated powdered
202 charcoal (activated Charcoal for analysis, Panreac Química, Barcelona, Spain) at a mass
203 ratio of hydrolyzate: activated charcoal of 1, 2.5 or 5% (w/v) at a temperature of 30ºC with
204 stirring at 150 rpm (Orbital shaking incubators, WY-100, Comecta S.A., distributed by
205 Scharlab, Madrid, Spain) for 12 h. Liquors were recovered by means of filtration (Bustos
206 Vázquez et al. 2017), diluted with distilled water 1/1 (v/v) and sterilized by autoclave
207 (Trade Raypa SL, Terrassa, Barcelona) at 121 ºC during 15 min.
208 Fermentations were done in 250 mL Erlenmeyer flasks containing 100 mL of raw or
209 detoxified neutralized hemicellulosic hydrolyzates supplemented with the nutrients of
210 MRS medium except glucose, and placed in orbital shakers at 150 rpm and 30°C
211 Samples (2 mL) were taken at given fermentation and filtered with 0.22 μm pore size
212 filters. The supernatants were frozen for subsequent analyses.
213 Fermentations and measurements were done in triplicate, and the means are reported. The
214 global volumetric productivities (Q_P) were calculated for the fermentation times
215 corresponding to the transition from high to low slope of the sigmoidal lactic acid profiles.
216
217 **2.9. Analytical methods**
218 Glucose, xylose, arabinose and acetic acid were measured through HPLC (Agilent, model
219 1200, Palo Alto, CA) using a refractive index detector with an Aminex HPX-87H ion
220 exclusion column (Bio Rad 300 × 7.8 mm, 9 μ particles) with a guard column, eluted with
221 0.003 M of sulfuric acid at a flow rate of 0.6 mL min^{-1} at 50ºC. Five μL of diluted samples
222 were injected, and after this, concentrations were obtained using the corresponding

223 calibration curve. Furfural and HMF were analyzed using a reverse phase HPLC system
224 (Agilent model 1200, Palo Alto, CA, USA) with a UV-diode array detector and a 4.6x150
225 mm Zorbax SB-Aq column (Agilent, Palo Alto, CA, USA) following the elution program
226 described by Paz et al. (2016). The identification of compounds was achieved by
227 combining the spectrum of each molecule with its retention time. Quantification was
228 performed through extrapolating the peak areas using the equation from the corresponding
229 standard curves.
230 Total phenolic content was determined by the Folin-Ciocalteu method (Singleton, V L. and
231 Rossi, 1965). Briefly, 0.5 mL of the sample was mixed with 3.75 mL of distilled water and
232 0.25 mL of Folin reagent previously diluted in distilled water (1:1 v/v). Then, 0.5 mL of
233 sodium carbonate (10% w/v) was added. The mixture was vigorously stirred and incubated
234 for 1h at room temperature. Samples were measured at 765 nm absorbance against a blank.
235 The content of total phenols was calculated in gallic acid equivalents using a calibration
236 curve (0-1 g L^{-1}).
237 Color intensity was analyzed in a supernatant using a UV-Vis Spectrophotometer (Libra
238 S60-Biochrom, Cambridge, U.K.) at an absorbance wavelength of 276 nm. Prior to the
239 measurement, samples were diluted to get a maximum absorbance wavelength value close
240 to 1.0.
241 The percentage of decolorization (D %) was calculated as follows equation:
242 $$D(\%) = \frac{A_{raw} - A_{detoxified}}{A_{raw}} \; x \; 100 \qquad \text{(Eq. 4)}$$
243 Where A_{raw} was the absorbance value of the raw hydrolyzate and $A_{detoxified}$ was the
244 absorbance value after each detoxification treatment.
245 **2.10. Statistical analysis**
246 The data obtained were analyzed with the statistical package SPSS Statistics® (version
247 19.0, SPSS Inc., Chicago, IL, USA), performing T tests for the equality of means (t-

248 Student) where necessary. A value of $p < 0.05$ was considered significant. Each value in
249 the graphs was expressed as mean ± Standard Deviation (SD) of three independent
250 experiments, conducted in triplicates.
251 On the hand, data tables 1 and 2 were analyzed with Statgraphics Centurion XVI (Version
252 16.1.11). The method currently being used to discriminate among the means is Tukey's
253 honestly significant difference (HSD) procedure. With this method, there is a 5,0 % risk of
254 calling one or more pairs significantly different when their actual difference equals 0.
255

256 **3. Results and discussion**

257 **3.1. Chemical composition of materials**

258 **Table 1** shows the compositional analysis of the selected chestnut wastes (leaves, prunings
259 and burrs of chestnut trees, and chestnut shells). The elemental analysis (content in C and
260 N) reveals that the carbon content is similar among samples, ranging between 42.8-47.3%.
261 However, it is worth noting that there is a higher nitrogen content for the prunings (1.4 ±
262 0.0), doubling the value attained for the other materials.
263 Regarding the mineral content of the samples, the amount of Zn found in chestnut prunings
264 (83.9 ± 1.6 mg kg^{-1}) is notable, being 10 times higher than in the other samples. Something
265 similar happens with Cu, where the content observed in prunings (9.0 ± 0.2 mg kg^{-1}) is
266 clearly higher. On the contrary, leaves showed higher levels of Na, K, Al and Mn.
267 Meanwhile, Ca, Mg and Fe were found in different proportions without being of particular
268 note in any one material. The remaining minerals (Si, Cr, Ni and Pb) were not quantified,
269 with the exception of 1.4 ± 0.1 mg kg^{-1} of Ni in prunings.
270 Table 1 also shows their polymeric content: percentages of glucan, xylan and arabinan.
271 Therefore, two types of material can be clearly differentiated. Leaves and shells are
272 characterized by their low percentages of glucan (16.54 ± 0.21 and 14.87 ± 0.16 %

273 respectively), xylan (11.68 ± 0.14 and 10.04 ± 0.16 % respectively) and arabinan (2.97 ±
274 0.10 and 2.91 ± 0.10 % respectively), without significant differences between them ($p > 0.05$), and were discarded due to being of little use for the production of sugars solutions.
276 In addition, these wastes showed a higher presence of Klason lignin (37.54 ± 0.37 and
277 44.31 ± 1.03%, respectively), which might also limit the generation of culture media,
278 independently of whether the chemical composition of lignin (its compositional
279 monomers) might be a more significant determinant than its amount for lignocellulose
280 recalcitrance during the pretreatment (Gall et al. 2017; Kim et al. 2017). On the other hand,
281 burrs and prunings show higher polysaccharide content, with significant different ($p < 0.05$) regarding the other materials, and relatively low lignin values. In particular, the
283 higher content of glucan (34.39 ± 2.1%) and xylan (21.34 ± 1.3%) found in burrs, along
284 with the lower amount of Klason lignin (22.61 ± 1.1%), makes burr wastes the most
285 promising for carrying out the subsequent stages of acid hydrolysis.
286 Few studies in the literature provide information on the chemical composition of these
287 materials. For instance, Vázquez et al. (2008) observed lower values of glucan (19.23%)
288 and higher content of acid-insoluble lignin (29.15%) during the characterization of
289 chestnut (*Castanea sativa*) shells. The compositional differences can be ascribed to the
290 inherent properties of the lignocellulosic materials, such as the origin of the material, the
291 geographical location and growth conditions, as well as the type of tissue analyzed.

292 **3.2. Influence of time on the chemical processing of chestnut burrs**

293 When a raw material is subjected to a mild hydrolysis with diluted acids (prehydrolysis),
294 what is obtained is a solution rich in hemicellulosic sugars, mainly xylose, and a solid
295 residue containing the untreated cellulose and lignin. The optimization of this treatment
296 usually adjusts process parameters such as temperature, acid concentration, liquid-to-solid
297 ratio and the reaction time, which must be changed according to the target biomass to

298 obtain the maximum yield of sugars and a minimum formation of toxic compounds (Brito
299 et al. 2018). Therefore, depending on the duration of the hydrolysis, some acetic acid
300 liberated from the acetyl groups of the material may also appear, as well as smaller
301 amounts of furfural and HMF generated by the dehydration of pentoses and hexoses,
302 respectively. These compounds are toxic inhibitors on microbial metabolism (Brito et al.
303 2018). Considering that one of the parameters to set is the time of hydrolysis, Table 2
304 shows the data obtained after the treatments carried out with 3% (w/v) H_2SO_4 at 15, 30 and
305 60 minutes. As can be seen, prehydrolysis results in the solubilization of sugars, with the
306 highest values, 23.48 ± 0.16 g L^{-1} xylose, 6.69 ± 0.02 g L^{-1} glucose and 3.31 ± 0.05 g L^{-1}
307 arabinose, being attained at an intermediate treatment time (30 min). In addition, when
308 reaction times increased at 60 min, a slight increase, with significant difference ($p < 0.05$)
309 is observed in the amount of furfural (0.64 ± 0.02 g L^{-1}) and HMF (0.17 ± 0.01 g L^{-1}).
310 Hence, the time of 30 minutes was chosen for the experimental design. This value is
311 intermediate of those reported in literature depending on the material studied. For instance,
312 Bustos et al. (2004) reported best operational conditions using 3% H_2SO_4 during only 15
313 min during the production of fermentable media from vine-trimming wastes; meanwhile
314 harsher conditions were necessary for acid pre-treatment of palm press fiber with a view to
315 the release of reducing sugars: 5.33% (w/v) H_2SO_4 and a hydrolysis time of 61.49 min
316 (Brito et al. 2018).

317 **3.3. Box–Behnken response surface methodology**

318 Acid hydrolysis also depends on other parameters, such as temperature and percentage of
319 acid. Because the study of the individual effects of each condition requires a large amount
320 of experimental work, a factorial design was carried out to simplify the experimentation
321 (Rivera et al., 2007). Several research groups have used phenomenological models based

on experimental designs to study the chemical processing and/or bioconversion of lignocellulosic materials (Bustos Vázquez et al., 2017; Salgado et al., 2015).

Table 3 shows the set of experimental conditions assayed (expressed in terms of coded variables) as well as the experimental data obtained for dependent variables y_1 to y_6. The sequence for the experimental work was randomly established to limit the influence of systematic errors. Experiments 10–12 are additional replications in the central point of the design (experiment 5) to measure the experimental error.

The quality of the developed models was evaluated based on the coefficient of determination (R^2) and the adjusted coefficient of determination (R^2 adjust). Table 4 shows this information. The worst results were achieved with variable y_2 (xylose), in which the coefficients were 0.93 and 0.88 respectively, indicating that 93% of the xylose released was attributed to the experimental variables studied, and the model could only fail to explain 7%. Table 4 also provides the ANOVA analysis that we used to determine the significance of the developed quadratic model by the lack of fit test. Lack of fit is a diagnostic test that compares the pure error based on the replicate measurements and shows the adequacy of the model. A *p*-value higher than 0.05 indicates that lack of fit is insignificant and hence determines that the quadratic model was valid for the study in question, whereas significant results means that the variation of the replicates in relation to their mean values is less than the variation of the design points about their predicted values. The drawback of this model is that it does not provide a good prediction when the runs replicate well and their variance is small. This was seen with HMF, in the pure error here of 0.00. In this case, the accuracy of the model was validated based on R^2 value (0.98) (Nasirizadeh et al. 2012; Vera Candioti et al. 2014). Finally, Table 4 also provides probability F-test and *p*-values to estimate the significance of each term. Large F-values

show that the variation can be explained by the developed regression equation. On the other hand, *p*-values lower than 0.05 indicate the statistically significant terms.

A Pareto chart was made (Figure 1) to visualize the contribution of each standardized effect on the release of compounds. In these figures, each bar is proportional to the estimated effect, and the vertical line (*p*-value = 0.05) is used to evaluate those effects which are statistically significant at a 95% confidence level. Six mathematical models were obtained to predict the different compounds released (y_i), in which those terms that are not statistically significant for the treatment ($p < 0.05$) were excluded for the regression equations, and presented as:

$$y_1 = 2.197184 + 1.440508x_1 + 0.523003x_2 - 0.166122x_1^2 + 0.225855x_2^2 + 0.372181x_1x_2 \quad \text{(Eq. 5)}$$

$$y_2 = 13.47660 + 7.63710x_1 + 3.79282x_2 \quad \text{(Eq. 6)}$$

$$y_3 = 3.507738 + 0.246743x_1 - 0.104474x_2 + 0.092454x_2^2 - 0.385898x_1x_2 \quad \text{(Eq. 7)}$$

$$y_4 = 3.642401 + 1.164617x_1 + 0.856982x_2 + 0.351834x_2^2 - 0.528887x_1x_2 \quad \text{(Eq. 8)}$$

$$y_5 = 0.202157 + 0.219017x_1 + 0.139961x_2 - 0.058166x_1^2 + 0.142579x_1x_2 \quad \text{(Eq. 9)}$$

$$y_6 = 0.082680 + 0.060322x_1 + 0.017620x_2 - 0.011711x_1^2 - 0.013790x_2^2 \quad \text{(Eq. 10)}$$

The positive coefficients of both linear independent variables (with the exception of Eq.6) indicate that high temperatures (x_1) and percentages of acid (x_2) within the studied range favored the release of all the compounds. The negative quadratic effect observed in temperature (x_1^2) in Eq.4 can be interpreted as, beyond the maximum point, the dehydration of glucose is promoted by sulfuric acid to produce 5-hydroxymethylfurfural (Brito et al. 2018).

Figure 2 shows 3D surface plots of the predicted dependence of dependent variables (y_i) on the operational variables (T and % H_2SO_4) generated on the base of the second-order polynomial equation. As a general trend, the curvatures of these plots show the effect of interaction, and the remarkable increases with the harsher conditions (defined by high

values of temperature and/or % H_2SO_4). Furthermore, the curvature of temperature (x_1) is less pronounced, and in particular temperature shows no influence under the harder concentrations of acid. Additionally, under lower concentrations of acids, temperature was not influential in variables y_1 (glucose) and y_5 (furfural), hardly influential in variable y_6 (HMF), and indeed was detrimental in variable y_3 (arabinose). Hence, the effect of sulfuric acid was more relevant in general.

3.4. Optimization of the operational condition y_2 (xylose concentration) and validation of the model

Under the severest conditions considered (130ºC and 5% H_2SO_4), the model predicted the released of up to 24.9 g L^{-1} of xylose. However, when using the desirability option from the Statistic software package, the value predicted (see Figure 3) was y_2 = 22.60 g L^{-1} of xylose, this being achieved when x_1 = 1 and x_2 = 0.5, corresponding to 130ºC and 3% (w/v) H_2SO_4, respectively.

In order to validate the model, a new experience was carried out in triplicate under the optimal conditions obtained when applying the desirability option, and the results obtained were: 6.91 ± 0.11 g L^{-1} glucose, 22.31 ± 0.12 g L^{-1} xylose, 3.32 ± 0.21 g L^{-1} arabinose, 5.02 ± 0.31 g L^{-1} acetic acid, 0.70 ± 0.01 g L^{-1} furfural and 0.20 ± 0.01 g L^{-1} HMF.

As can be seen, the value obtained for xylose (22.31 ± 0.12 g L^{-1}) is similar to the 22.60 g L^{-1} predicted by the model, and thus it can be considered an appropriate model.

3.5. Neutralization and detoxification of hemicellulosic hydrolyzates

Acid hydrolysis releases not only the monomeric sugars susceptible to be fermented (glucose, xylose and arabinose), but also several microbial inhibitors, which can cause inhibition of microbial metabolism and reduce cell growth and product yield, including low-molecular-weight phenolic compounds, furan derivatives such as furfural, HMF, aliphatic acids such as formic acid, levulinic acid, and acetic acid, or even minerals/metals

contained in the lignocellulosic materials or resulting from the corrosion of the hydrolysis equipment (Bustos Vázquez et al. 2017; Lee et al. 2011). In this study we have focused on three types of inhibitors: aliphatic acids (acetic acid), furan derivatives (furfural and HMF) and phenolic compounds.

In our case, the acid hemicellulosic hydrolyzate obtained under optimized conditions exhibited a dark color and the following composition: aliphatic acids (5.00 ± 0.26 g L^{-1} acetic acid), furans (0.65 ± 0.00 g L^{-1} furfural and 0.19 ± 0.00 g L^{-1} HMF) and phenolic compounds (2.38 g L^{-1} equivalent to gallic acid), making the hydrolyzate unsuitable for microbial growth (Behera et al., 2014; Chandel et al., 2013; Palmqvist, 2000). Acetic acid formation is mainly due to the degradation of the hemicellulose glucuronoxylan, where acetyl groups (at carbon 2 or 3 of the glucuronoxylan backbone) are cleaved (Lee et al. 2011). When acetic acid and formic acid (a degradation product of HMF) enter in the cell in the undissociated form, they become dissociated in the protoplasm because of its pH, leading to a decrease in the intracellular pH that can generate cell death (Mateo et al., 2013). Phenolic compounds cause the loss of integrity of biological membranes, thereby affecting their ability to serve as selective barriers and enzyme matrices (Brito et al. 2018; Mateo et al. 2013). The furans derivatives furfural and HMF are formed by the hydrolysis of pentoses and hexoses, respectively. *In vitro* evaluations have shown that furans directly inhibit alcohol dehydrogenase (ADH), pyruvate dehydrogenase (PDH) and aldehyde dehydrogenase (ALDH) and cause acetaldehyde accumulation which subsequently prolongs the lag-phase of fermenting microorganisms (Gupta et al., 2017).

Consequently, three dosages of activated charcoal (1, 2.5 and 5% w/v) were assayed to detoxify the neutralized hydrolyzate. Activated charcoal has been assayed widely in different hemicellulosic liquors. For instance, Brito et al. (2018) reduced the content of total phenolic compounds, furfural and HMF in palm press fiber hemicellulosic

hydrolyzates using 5% (w/v) activated charcoal from 0.66 ± 0.03 g L^{-1}, 489.50 mg L^{-1} and 46.14 mg L^{-1} to 0.06 ± 0.01 g L^{-1}, 3.37 mg L^{-1} and undetected, respectively. Lee et al. (2011) using 2.5% activated carbon in autohydrolysis prehydrolyzate from mixed hardwood chips, were able to remove 42% of formic acid, 14% of acetic acid, 96% of HMF and 93% of the furfural, although they also removed 8.9% of sugars. Mateo et al. (2013) also decreased inhibitors from olive tree pruning residue hydrolyzates (removing 46% of acetic acid, 81% of phenolic compounds and 98% of total furans) with 2% charcoal. Meanwhile Morana et al. (2017), with 5% (w/v) activated charcoal and repeated adsorption-desorption processes, enabled the recovery of 70.3% (w/w) of phenolic compounds in chestnut shell hydrolyzates, whilst simultaneously retaining the soluble sugars in the detoxified hydrolyzate.

Figure 4 shows the color removal at different activated charcoal dosages. It can be observed that, independently of the amount of charcoal assayed, a high color removal rate was reached up to 2 h, and then equilibrium was reached. This tendency can be interpreted in light of the high initial number of sites in activated charcoal, hence the greater driving force for the mass transfer and consequently the phenolic compounds reacted easily at adsorption sites. After 2 h, the number of free sites decreased and the non-adsorbate molecules were assembled at the surface, thus limiting the capacity of adsorption (Gupta et al., 2017).

On the other hand, Table 5 shows the amounts of monosaccharides released, as well as those toxic compounds present in the raw hydrolyzate and the liquors obtained after detoxification with activated charcoal under different dosages. A clear increase can be observed in the amount of substances removed with the increase of charcoal, with the exception of acetic acid, which remained constant. Brito et al. (2018) also observed an increment of acetic acid from 12.02 to 16.65 g L^{-1} after the treatment with 5% (w/v)

448 activated charcoal. On the positive side, the concentration of sugars was only slightly
449 reduced with the increase of charcoal assayed. Conversely, Brito et al. (2018) observed
450 that treatment with activated charcoal resulted in an increase in the concentration of the
451 reducing sugars from 83.1 to 94.9 g L^{-1} in the hydrolyzate. A similar increase was also
452 observed by Díaz et al. (2009) with 5% (w/v) activated charcoal, the authors here
453 concluding that the increase in sugar concentration occurred as a result of the evaporation
454 of water during the treatment, which required heating at 50ºC for 60 min. However, this
455 cannot be applied to our results since the process was carried out at room temperature.

456 The most important finding was that furan derivatives and phenolic compounds underwent
457 the highest percentages of elimination. Thus, using 1% charcoal, the amounts of phenolic
458 compounds decreased from 2.38±0.00 g L^{-1} in raw hydrolyzates to 0.27 ± 0.00 g L^{-1} and up
459 to 0.02 ± 0.00 g L^{-1} with 5%, with percentages of color removal of 51.30 ± 0.28 and
460 95.27±0.03 %, respectively. Similarly, furfural was completely removed with 2.5%
461 charcoal, and HMF was reduced from 0.06±0.00 g L^{-1} in raw hydrolyzates to 0.02±0.00 g
462 L^{-1} in hydrolyzates detoxified at the highest level (5%).

463 **3.6. Fermentation of neutralized hemicellulosic hydrolyzates**

464 In order to assay the fermentability of hemicellulosic hydrolyzates, three fastidious-
465 growing microorganisms *Lactococcus lactis* subsp. *lactis* CECT 4434, *Lactobacillus*
466 *pentosus* CECT 4023 and *Lactobacillus plantarum* CECT 221 were cultivated separately
467 for 36h in raw or detoxified neutralized hemicellulosic hydrolyzates. In all cases, a
468 prolonged lag period was observed (data not shown). Consequently, hydrolyzates were
469 diluted with distilled water in the proportion 1/1 (v/v) in order to reduce the toxic effect of
470 inhibitory compounds. Therefore, a new set of experiments was carried out using diluted
471 hydrolyzates. In this case, it was observed the complete absence of sugars (glucose, xylose
472 and arabinose) consumption, and consequently the negligible production of lactic acid and

acetic acid when the strains were grown in raw diluted hemicellulosic hydrolyzates (left column of **Figure 5**). Conversely, all the strains produced different amounts of lactic acid when detoxified diluted acid hydrolyzates were assayed. **Table 6** shows the stoichiometric parameters, productivities and yields for bioconversion assays. The best results were obtained with the strain *L. plantarum*, since a regular increase in lactic acid was quantified till 12h, remaining almost constant thereafter. The maximum lactic acid production was 6.85 g/L, corresponding to a global volumetric productivity of lactic acid (Q_P) of 0.51 g/L·h; a sugars consumption rate (Q_S) of 0.58 g/L·h; and a product yield ($Y_{P/S}$) of 0.89 g/g. *L. pentosus* showed a similar tendency, although the growth was slightly slower, being necessary 20h to reach a highest lactic acid concentration of 6.56 g/L (Q_P = 0.29 g/L·h; Q_S = 0.32 g/L·h and $Y_{P/S}$ = 0.92 g/g). Finally, although *L. lactis* experienced the lowest production, 4.15 g/L lactic acid was obtained after 20h (Q_P = 0.18 g/L·h; Q_S = 0.21 g/L·h and $Y_{P/S}$ = 0.83 g/g). On the other hand, acetic acid, the main by-product of fermentation hardly increased in all experiments. The lactic acid yields superior to 0.83 g/g calculated with the three strains confirm the suitability of detoxified neutralized hemicellulosic hydrolyzate of chestnut burrs as culture broths to carry out fermentative processes.

Conclusions

Chestnut wastes are produced in large amounts worldwide. However, these agroindustrial by-products are undervalued. Due to their lignocellulosic character, they could be used as an economic feedstock for biorefinery processes. The higher content of glucan and xylan found in chestnut burrs, along with the lower amount of Klason lignin, makes this waste the most promising for carrying out the subsequent stages of acid hydrolysis. Hydrolysis catalyzed by dilute sulfuric acid (prehydrolysis) is a suitable technology to recover hemicellulosic sugars, particularly xylose. Intermediate treatment time (30 min) resulted in the highest amounts of sugars released. Operating under selected operational conditions

(130ºC and 3% (w/v) H_2SO_4), high amounts of xylose can be produced, being sulfuric acid more relevant than temperature. However, some inhibitory compounds were also present in the hemicellulosic liquor, including aliphatic acids, furans, and phenolic compounds. Therefore, detoxification with 5% charcoal led to almost complete removal of color and phenolic compounds, making this hydrolyzate a good candidate for the production of culture media suitable for microbial growth under a wide range of microorganisms. This hypothesis was corroborated by growing successfully three lactic acid bacteria in spite of their high requirements to be fermented.

Acknowledgments

The development of this project is financed by the Galician Innovation Agency (Project: Valorización de residuos agroindustriales para la obtención de bioproductos de alto valor añadido "Innobiorresiduos") and co-financed by 80% by the European Regional Development Fund under the Feder Galicia 2014-2020 operational program (OT 1. "Promote technological development, innovation and quality research").

Declarations of interest: none

4. Bibliografía

Aires, A., Carvalho, R., José, M., 2016. Valorization of solid wastes from chestnut industry processing : Extraction and optimization of polyphenols , tannins and ellagitannins and its potential for adhesives , cosmetic and pharmaceutical industry. Waste Manag. 48, 457–464. https://doi.org/10.1016/j.wasman.2015.11.019

Alves de Oliveira, R., Komesu, A., Vaz Rossell, C.E., Wolf Maciel, M.R., Maciel Filho, R., 2019. Concentrating second-generation lactic acid from sugarcane bagasse via hybrid short path evaporation: Operational challenges. Sep. Purif. Technol. 209, 26–31. https://doi.org/10.1016/j.seppur.2018.07.012

Arevalo-gallegos, A., Ahmad, Z., Asgher, M., Parra-saldivar, R., Iqbal, H.M.N., 2017. International Journal of Biological Macromolecules Lignocellulose : A sustainable material to produce value-added products with a zero waste approach — A review. Int. J. Biol. Macromol. 99, 308–318. https://doi.org/10.1016/j.ijbiomac.2017.02.097

Behera, S., Arora, R., Nandhagopal, N., Kumar, S., 2014. Importance of chemical pretreatment for bioconversion of lignocellulosic biomass. Renew. Sustain. Energy Rev. 36, 91–106. https://doi.org/10.1016/j.rser.2014.04.047

Bhowmick, G. De, Sarmah, A.K., Sen, R., 2018. Bioresource Technology Lignocellulosic biore fi nery as a model for sustainable development of biofuels and value added products. Bioresour. Technol. 247, 1144–1154. https://doi.org/10.1016/j.biortech.2017.09.163

Brito, P.L., de Azevedo Ferreira, C.M., Silva, A.F.F., Pantoja, L. de A., Nelson, D.L., dos Santos, A.S., 2018. Hydrolysis, Detoxification and Alcoholic Fermentation of Hemicellulose Fraction from Palm Press Fiber. Waste and Biomass Valorization 9, 957–968. https://doi.org/10.1007/s12649-017-9882-4

Bustos, G., Arcos, U., Vecino, X., Cruz, J.M., Moldes, A.B., 2018. Recycled Lactobacillus pentosus biomass can regenerate biosurfactants after various fermentative and extractive cycles. Biochem. Eng. J. 132, 191–195. https://doi.org/10.1016/j.bej.2018.01.021

Bustos Vázquez, G., Pérez-Rodríguez, N., Salgado, J.M., Oliveira, R.P.D.S., Domínguez, J.M., 2017. Optimization of Salts Supplementation on Xylitol Production by Debaryomyces hansenii Using a Synthetic Medium or Corncob Hemicellulosic Hydrolyzates and Further Scaled Up. Ind. Eng. Chem. Res. 56, 6579–6589. https://doi.org/10.1021/acs.iecr.7b01120

Chandel, A.K., Silvério, S., Singh, O. V, 2013. Detoxification of Lignocellulose Hydrolysates : Biochemical and Metabolic Engineering Toward White Biotechnology 388–401. https://doi.org/10.1007/s12155-012-9241-z

da Silva Sabo, S., Pérez-Rodríguez, N., Domínguez, J.M., de Souza Oliveira, R.P., 2017. Inhibitory substances production by Lactobacillus plantarum ST16Pa cultured in hydrolyzed cheese whey supplemented with soybean flour and their antimicrobial efficiency as biopreservatives on fresh chicken meat. Food Res. Int. 99, 762–769. https://doi.org/10.1016/j.foodres.2017.05.026

Díaz, M.J., Ruiz, E., Romero, I., Cara, C., Moya, M., Castro, E., 2009. Inhibition of Pichia stipitis fermentation of hydrolysates from olive tree cuttings. World J. Microbiol. Biotechnol. 25, 891–899. https://doi.org/10.1007/s11274-009-9966-9

FAOSTAT. URL http://www.fao.org/faostat/en/#data (accessed 5.27.18).

Gupta, R., Hemansi, Gautam, S., Shukla, R., Kuhad, R.C., 2017. Study of charcoal detoxification of acid hydrolysate from corncob and its fermentation to xylitol. J. Environ. Chem. Eng. 5, 4573–4582. https://doi.org/10.1016/j.jece.2017.07.073

Karasu-yalcin, K.E.S., 2016. Evaluation of some lignocellulosic byproducts of food

564 industry for microbial xylitol production by Candida tropicalis. 3 Biotech 6, 1–7.
565 https://doi.org/10.1007/s13205-016-0521-8
566 Mateo, S., Conceic, I., Sánchez, S., Moya, A.J., 2013. Detoxification of hemicellulosic
567 hydrolyzate from olive tree pruning residue 49, 196–203.
568 https://doi.org/10.1016/j.indcrop.2013.04.046
569 Morana, A., Squillaci, G., Paixão, S.M., Alves, L., La Cara, F., Moura, P., 2017.
570 Development of an energy biorefinery model for chestnut (Castanea sativa Mill.)
571 shells. Energies 10, 1–14. https://doi.org/10.3390/en10101504
572 Myoung, J., Venditti, R.A., Jameel, H., Kenealy, W.R., 2010. Detoxification of woody
573 hydrolyzates with activated carbon for bioconversion to ethanol by the thermophilic
574 anaerobic bacterium Thermoanaerobacterium saccharolyticum. Biomass and
575 Bioenergy 35, 626–636. https://doi.org/10.1016/j.biombioe.2010.10.021
576 Nasirizadeh, N., Dehghanizadeh, H., Yazdanshenas, M.E., Moghadam, M.R., Karimi, A.,
577 2012. Optimization of wool dyeing with rutin as natural dye by central composite
578 design method. Ind. Crops Prod. 40, 361–366.
579 https://doi.org/10.1016/j.indcrop.2012.03.035
580 Palmqvist, E., 2000. Fermentation of lignocellulosic hydrolysates . II : inhibitors and
581 mechanisms of inhibition 74, 25–33.
582 Paz, A., Carballo, J., Pérez, M.J., Domínguez, J.M., 2016. Bacillus aryabhattai BA03: a
583 novel approach to the production of natural value-added compounds. World J.
584 Microbiol. Biotechnol. 32. https://doi.org/10.1007/s11274-016-2113-5
585 Paz, A., da Silva Sabo, S., Vallejo, M., Marguet, E., Pinheiro de Souza Oliveira, R.,
586 Domínguez, J.M., 2018. Using brewer's spent grain to formulate culture media for the
587 production of bacteriocins using Patagonian strains. Lwt 96, 166–174.
588 https://doi.org/10.1016/j.lwt.2018.05.027
589 Picchi, G., Lombardini, C., Pari, L., Spinelli, R., 2018. Physical and chemical
590 characteristics of renewable fuel obtained from pruning residues. J. Clean. Prod. 171,
591 457–463. https://doi.org/10.1016/j.jclepro.2017.10.025
592 Portilla Rivera, O.M., Arzate Martínez, G., Jarquín Enríquez, L., Vázquez Landaverde,
593 P.A., Domínguez González, J.M., 2015. Lactic Acid and Biosurfactants Production
594 from Residual Cellulose Films. Appl. Biochem. Biotechnol. 177, 1099–1114.
595 https://doi.org/10.1007/s12010-015-1799-4
596 Rivera, O.M.P., Moldes, A.B., Torrado, A.M., Domínguez, J.M., 2007. Lactic acid and
597 biosurfactants production from hydrolyzed distilled grape marc. Process Biochem. 42,
598 1010–1020. https://doi.org/10.1016/j.procbio.2007.03.011
599 Rodríguez-Pazo, N., Da Silva Sabo, S., Salgado-Seara, J.M., Arni, S. Al, De Souza
600 Oliveira, R.P., Domínguez, J.M., 2016. Optimisation of cheese whey enzymatic
601 hydrolysis and further continuous production of antimicrobial extracts by
602 Lactobacillus plantarum CECT-221. J. Dairy Res. 83, 402–411.
603 https://doi.org/10.1017/S0022029916000352
604 Salgado, J.M., Abrunhosa, L., Venâncio, A., Domínguez, J.M., Belo, I., 2015. Enhancing
605 the Bioconversion of Winery and Olive Mill Waste Mixtures into Lignocellulolytic
606 Enzymes and Animal Feed by Aspergillus uvarum Using a Packed-Bed Bioreactor. J.
607 Agric. Food Chem. 63, 9306–9314. https://doi.org/10.1021/acs.jafc.5b02131
608 Santos, J., Antorrena, G., Freire, M.S., Pizzi, A., González-Álvarez, J., 2017.
609 Environmentally friendly wood adhesives based on chestnut (Castanea sativa) shell
610 tannins. Eur. J. Wood Wood Prod. 75, 89–100. https://doi.org/10.1007/s00107-016-
611 1054-x
612 Seong, H.A., Lee, J.S., Yoon, S.Y., Song, W.Y., Shin, S.J., 2016. Fermentation
613 characteristics of acid hydrolysates by different neutralizing agents. Int. J. Hydrogen

Energy 41, 16365–16372. https://doi.org/10.1016/j.ijhydene.2016.05.003
Singleton, V L.; Rossi Jr, J.A., 1965. Colorimetry of Total Phenolics with Phosphomolybdic-Phosphotungstic Acid Reagents. Am. J. Enol. Vitic. 16, 144–158. https://doi.org/10.12691/ijebb-2-1-5
Smichi, N., Messaoudi, Y., Gargouri, M., 2018. Lignocellulosic Biomass Fractionation : Production of Ethanol , Lignin and Carbon Source for Fungal Culture. Waste and Biomass Valorization 9, 947–956. https://doi.org/10.1007/s12649-017-9859-3
Vázquez, G., Fernández-Agulló, A., Gómez-Castro, C., Freire, M.S., Antorrena, G., González-Álvarez, J., 2012. Response surface optimization of antioxidants extraction from chestnut (Castanea sativa) bur. Ind. Crops Prod. 35, 126–134. https://doi.org/10.1016/j.indcrop.2011.06.022
Vázquez, G., Fontenla, E., Santos, J., Freire, M.S., González-Álvarez, J., Antorrena, G., 2008. Antioxidant activity and phenolic content of chestnut (Castanea sativa) shell and eucalyptus (Eucalyptus globulus) bark extracts. Ind. Crops Prod. 28, 279–285. https://doi.org/10.1016/j.indcrop.2008.03.003
Ventorino, V., Parillo, R., Testa, A., Viscardi, S., Espresso, F., Pepe, O., 2016. Chestnut green waste composting for sustainable forest management : Microbiota dynamics and impact on plant disease control. J. Environ. Manage. 166, 168–177. https://doi.org/10.1016/j.jenvman.2015.10.018
Vera Candioti, L., De Zan, M.M., Cámara, M.S., Goicoechea, H.C., 2014. Experimental design and multiple response optimization. Using the desirability function in analytical methods development. Talanta 124, 123–138. https://doi.org/10.1016/j.talanta.2014.01.034

654 **Table 1.** Characterization of raw materials.

	Chestnut leaves	**Chestnut burrs**	**Chestnut pruning**	**Chestnut shells**
C (%)	47.3 ± 0.2	42.8 ± 0.2	45.0 ± 0.1	46.6 ± 0.5
N (%)	0.6 ± 0.0	0.6 ± 0.0	1.4 ± 0.0	0.7 ± 0.0
Ca (g kg^{-1})	5.7 ± 0.4	1.1 ± 0.1	11.4 ± 1.1	1.3 ± 0.0
Mg (g kg^{-1})	2.7 ± 0.1	0.9 ± 0.0	3.5 ± 0.4	1.0 ± 0.1
Na (mg kg^{-1})	135.0 ± 2.8	29.7 ± 0.4	49.1 ± 2.3	47.4 ± 5.1
K (mg kg^{-1})	148.5 ± 3.5	32.7 ± 0.6	50.4 ± 3.3	48.9 ± 5.4
Al (mg kg^{-1})	434.7 ± 17.7	<300	<300	<300
Si (mg kg^{-1})	<300	<300	<300	<300
Zn (mg kg^{-1})	8.2 ± 0.1	5.8 ± 0.0	83.9 ± 1.6	6.8 ± 0.0
Fe (mg kg^{-1})	55.0 ± 0.4	20.7 ± 0.2	42.5 ± 1.2	11.4 ± 0.1
Mn (mg kg^{-1})	1737.8 ±24.9	184.9 ± 1.1	539.2 ± 11.1	122.4 ± 4.5
Cr (mg kg^{-1})	<1 (0.8)	<1	<1	<1
Ni (mg kg^{-1})	<1 (0.8)	<1 (0.8)	1.4 ± 0.1	<1
Cu (mg kg^{-1})	2.4 ± 0.0	2.4 ± 0.0	9.0 ± 0.2	2.9 ± 0.0
Pb (mg kg^{-1})	<1	<1	<1	<1
Humidity (%)	9.16 ± 0.04^{a}	11.24 ± 0.00^{b}	7.73 ± 0.00^{c}	10.37 ± 0.00^{d}
Ash (%)	2.82 ± 0.06^{a}	0.96 ± 0.03^{b}	4.08 ± 0.22^{c}	0.58 ± 0.10^{b}
Extracts (%)	8.98 ± 0.62^{a}	3.29 ± 0.08^{b}	6.68 ± 0.29^{c}	5.34 ± 0.40^{c}
ASL (%)	6.45 ± 0.28^{a}	$6.88 \pm 0.01^{a,b}$	$6.03 \pm 0.07^{a,c}$	3.90 ± 0.06^{d}
Klason lignin (%)	37.54 ± 0.37^{a}	22.62 ± 1.12^{b}	23.24 ± 0.12^{c}	44.31 ± 1.03^{d}
Glucan (%)	16.54 ± 0.21^{a}	34.39 ± 2.07^{b}	30.72 ± 0.20^{b}	14.87 ± 0.16^{a}
Xylan (%)	11.68 ± 0.14^{a}	21.35 ± 1.30^{b}	17.03 ± 0.13^{c}	10.04 ± 0.16^{a}
Arabinan (%)	2.97 ± 0.10^{a}	$3.05 \pm 0.01^{a,b}$	$2.52 \pm 0.11^{a,c}$	2.91 ± 0.10^{a}
Acetyl groups (%)	3.09 ± 0.17^{a}	$5.45 \pm 0.10^{a,b}$	$4.57 \pm 0.05^{a,c}$	3.04 ± 0.12^{a}

655 ASL: Acid soluble lignin. Same letters show no significant difference ($p > 0.05$).

656

Table 2. Compounds released (expressed in g L^{-1}) during the prehydrolysis stage carried out using 3% (w/v) H_2SO_4 at different times.

	15 min	**30 min**	**60 min**
Glucose	3.57 ± 0.03^{a}	4.25 ± 0.01^{b}	4.74 ± 0.11^{c}
Xylose	22.15 ± 0.13^{a}	23.48 ± 0.16^{b}	22.60 ± 0.13^{a}
Arabinose	3.30 ± 0.03^{a}	3.31 ± 0.05^{a}	3.02 ± 0.11^{a}
Acetic acid	5.36 ± 0.05^{a}	5.35 ± 0.10^{a}	5.50 ± 0.08^{a}
Furfural	0.43 ± 0.01^{a}	0.51 ± 0.01^{b}	0.64 ± 0.02^{c}
HMF	0.11 ± 0.01^{a}	0.15 ± 0.00^{b}	0.17 ± 0.01^{c}

HMF: hydroxymethylfurfural. Same letters show no significant difference ($p > 0.05$).

675 **Table 3.** Operational conditions considered in the hydrolysis of chestnut burrs, expressed in
676 terms of the coded independent variables x_1 (temperature) and x_2 (H_2SO_4 concentration) and
677 experimental results achieved after 30 minutes of hydrolysis for the dependent variables y_1
678 (glucose concentration, g L^{-1}), y_2 (xylose concentration, g L^{-1}), y_3 (arabinose concentration, g
679 L^{-1}), y_4 (AcH concentration, g L^{-1}), y_5 (furfural concentration, g L^{-1}) and y_6 (HMF
680 concentration, %).

	Operational conditions		**Experimental results**					
Exp	**T**	**%**	**Glucose**	**Xylose**	**Arabinose**	**AcH**	**Furfural**	**HMF**
1	-1	-1	0.86	0.37	3.01	0.94	0.02	0.03
2	-1	0	0.76	5.95	3.21	2.80	0.02	0.02
3	-1	1	0.98	9.91	3.50	3.43	0.03	0.04
4	0	-1	0.99	6.06	3.47	2.37	0.04	0.07
5	0	0	2.46	16.90	3.64	4.60	0.09	0.04
6	0	1	2.40	19.06	3.40	4.64	0.28	0.10
7	1	-1	2.72	19.83	4.18	4.35	0.15	0.13
8	1	0	6.69	22.17	3.89	5.08	0.50	0.14
9	1	1	4.33	20.05	3.13	4.73	0.73	0.19
10	0	0	2.14	14.37	3.70	3.94	0.08	0.03
11	0	0	2.37	17.58	3.74	4.47	0.11	0.05
12	0	0	2.39	17.63	3.75	4.32	0.12	0.05

681 AcH: acetic acid; HMF: hydroxymethylfurfural
682
683
684

685 **Table 4.** ANOVA for the second-order polynomial model and coefficients of determination.

y_1 (Glucose)						
Factor	**Sum of squares**	**Degree of freedom**	**Mean square**	**F-value**	***p*-value**	***Significant level***
x_1 (L+Q)	12.74	2	6.37	340.30	0.00	*
x_2 (L+Q)	2.19	2	1.09	58.35	0.00	*
x_1*x_2	0.55	1	0.55	29.59	0.01	**
Lack of Fit	0.43	3	0.14	7.73	0.06	
Pure Error	0.06	3	0.02			
Total SS	15.78	11				
R-sqr = 0.97; Adj: 0.94; MS Pure Error = 0.02						
y_2 (Xylose)						
Factor	**Sum of squares**	**Degree of freedom**	**Mean square**	**F-value**	***p*-value**	***Significant level***
x_1 (L+Q)	354.40	2	177.20	75.19	0.00	*
x_2 (L+Q)	107.06	2	53.53	22.71	0.01	**
x_1*x_2	21.74	1	21.74	9.23	0.05	
Lack of Fit	26.99	3	8.99	3.82	0.15	
Pure Error	7.07	3	2.36			
Total SS	527.62	11				
R-sqr = 0.93; Adj: 0.88; MS Pure Error = 2.36						
y_3 (Arabinose)						
Factor	**Sum of squares**	**Degree of freedom**	**Mean square**	**F-value**	***p*-value**	***Significant level***
x_1 (L+Q)	0.38	2	0.19	77.62	0.00	*
x_2 (L+Q)	0.16	2	0.08	32.23	0.00	*
x_1*x_2	0.59	1	0.59	245.12	0.00	*
Lack of Fit	0.06	3	0.02	8.37	0.06	
Pure Error	0.01	3	0.00			
Total SS	1.23	11				
R-sqr = 0.94; Adj: 0.90; MS Pure Error = 0.02						
y_4 (Acetic acid)						
Factor	**Sum of squares**	**Degree of freedom**	**Mean square**	**F-value**	***p*-value**	***Significant level***
x_1 (L+Q)	8.33	2	4.16	52.26	0.00	*
x_2 (L+Q)	5.73	2	2.86	35.93	0.00	*
x_1*x_2	1.12	1	1.12	14.04	0.03	*
Lack of Fit	0.27	3	0.09	1.15	0.45	
Pure Error	0.24	3	0.08			
Total SS	16.26	11				
R-sqr = 0.97; Adj: 0.94; MS Pure Error = 0.80						
y_5 (Furfural)						
Factor	**Sum of squares**	**Degree of freedom**	**Mean square**	**F-value**	***p*-value**	***Significant level***
x_1 (L+Q)	0.32	2	0.16	664.20	0.00	*
x_2 (L+Q)	0.12	2	0.06	242.22	0.00	*
x_1*x_2	0.08	1	0.08	333.50	0.00	*
Lack of Fit	0.01	3	0.00	9.49	0.05	**
Pure Error	0.00	3	0.00			
Total SS	0.54	11				
R-sqr = 0.98; Adj: 0.97; MS Pure Error = 0.00						
y_6 (HMF)						
Factor	**Sum of squares**	**Degree of freedom**	**Mean square**	**F-value**	***p*-value**	***Significant level***
x_1 (L+Q)	0.02	2	0.01	205.23	0.00	*
x_2 (L+Q)	0.00	2	0.00	34.28	0.01	*
x_1*x_2	0.00	1	0.00	7.96	0.06	**
Lack of Fit	0.00	3	0.00	1.90	0.30	
Pure Error	0.00	3	0.00			
Total SS	0.03	11				
R-sqr = 0.98; Adj: 0.97; MS Pure Error = 0.00						
Significant coefficients at the 99% confidence level (*) or 95% (**)						

686 **Table 5.** Chemical composition of the raw and detoxified hydrolyzates (with 1, 2.5 and 5%
687 (w/v) activated charcoal).

	Raw	1% (w/v)	2.5% (w/v)	5% (w/v)
Sugars and acids				
Glucose	5.15±0.10	4.15±0.01	3.90±0.00	3.53±0.08
Xylose	17.24±0.20	13.78±0.05	13.58±0.09	12.66±0.16
Arabinose	3.47±0.07	2.46±0.03	2.44±0.03	2.37±0.24
Oxalic acid	1.63±0.01	2.40±0.24	2.21±0.13	2.00±0.16
Tartaric acid	1.75±0.02	1.67±0.13	1.62±0.01	1.46±0.02
Aliphatic acids				
Acetic acid	4.16±0.14	4.45±0.09	4.22±0.00	4.13±0.09
Furan derivatives				
Furfural	0.25±0.02	0.04±0.01	n.d.	n.d.
HMF	0.06±0.00	0.05±0.00	0.03±0.00	0.02±0.00
Phenolic compounds				
Phenolic compounds*	2.38±0.00	0.27±0.00	0.10±0.00	0.02±0.00
% color removal	-	51.30±0.28	80.21±1.74	95.27±0.03

688 n.d.: not detected.
689 *expressed as equivalent to gallic acid

690

691

692

693

694

695

696

697

698

699

700 **Table 6.** Stoichiometric parameters (g L^{-1}), productivities and yields for bioconversion assays
701 carried out by *L. plantarum*, *L. pentosus* and *L. lactis* grown in raw or detoxified diluted
702 hemicellulosic hydrolyzates.

	L. plantarum		*L. pentsosus*		*L. lactis*	
	RHH	DHH	RHH	DHH	RHH	DHH
Glucose $_{\text{time 0}}$ (g/L)	4.66	4.38	4.86	4.42	4.82	4.33
Glucose $_{\text{time t}}$ (g/L)	4.62	1.47	4.50	2.06	4.98	2.03
Xylose $_{\text{time 0}}$ (g/L)	7.57	6.02	7.66	6.04	7.19	6.04
Xylose $_{\text{time t}}$ (g/L)	7.52	3.64	7.41	3.77	7.00	4.42
Arabinose $_{\text{time 0}}$ (g/L)	1.90	1.65	1.35	1.71	1.86	1.68
Arabinose $_{\text{time t}}$ (g/L)	1.96	0.00	1.97	0.00	2.01	1.32
Lactic acid $_{\text{time 0}}$ (g/L)	0.00	0.67	1.00	0.72	0.95	0.61
Lactic acid $_{\text{time t}}$ (g/L)	0.00	6.85	0.99	6.56	0.88	4.15
Acetic acid $_{\text{time 0}}$ (g/L)	8.75	6.32	6.50	6.35	6.68	6.22
Acetic acid $_{\text{time t}}$ (g/L)	7.08	6.94	6.75	6.79	6.90	5.98
Time (h)	36	12	36	20	36	20
Q_P (g/L·h)	0.00	0.51	0.00	0.29	0.00	0.18
Q_S (g/L·h)	0.00	0.58	0.00	0.32	0.00	0.21
$Y_{P/S}$ (g/g)	0.00	0.89	0.80	0.92	0.66	0.83

703 RHH: raw hemicellulosic hydrolyzates
704 DHH: detoxified hemicellulosic hydrolyzates
705 Time: fermentation times corresponding to the transition from high to low slope of the
706 sigmoidal lactic acid profiles
707 Q_P, global volumetric productivity of lactic acid
708 Q_S, sugars (glucose + xylose + arabinose) consumption rate
709 $Y_{P/S}$, lactic acid yield (g lactic acid produced g^{-1} sugars consumed).
710

711

712

713

714

715

716

717

718

719

720 **FIGURE LEGENDS**

Figure 1. Pareto chart for a) glucose, b) xylose, c) arabinose, d) acetic acid, e) furfural and f) HMF.

Figure 2. Dependence of a) glucose, b) xylose, c) arabinose, d) acetic acid, e) furfural and f) HMF on temperature (coded) and H_2SO_4 concentration (coded).

Figure 3 Profiles for predicted values and desirability model to determine optimum xylose released. Dashed lines indicate the optimization values.

Figure 4. Course with time of color removal using different concentrations of charcoal (w/v): 1% (■), 2.5% (●) and 5% (▲).

Figure 5. Profile of sugars consumption, and the production of lactic acid and acetic acid, by a) *L. plantarum*; b) *L. pentosus*; and c) *L. lactis* grown in raw diluted hemicellulosic hydrolyzates (left column) or diluted hemicellulosic hydrolyzates (right column) detoxified with 5% (w/v) charcoal: Glucose (♦), xylose (●), arabinose (×), lactic acid (■) and acetic acid (▲).

Valorization of chestnut (*Castanea sativa*) residues: characterization of different materials and optimization of the acid-hydrolysis of chestnut burrs for the elaboration of culture broths

Abstract

Four kinds of waste from the industrial processing of chestnuts (*Castanea sativa*), namely leaves, pruned material and burrs from chestnut tree plus chestnut shells, were characterized to determine their content in polymers and thus their potential use in biorefinery processes. Results revealed that chestnut burrs have the highest polysaccharide content being the most promising for carrying out the subsequent stages of acid hydrolysis. Treatment with diluted sulfuric acid (prehydrolysis) allowed the solubilization of xylose, glucose and arabinose, but also some toxic compounds such as furan derivatives, aliphatic acids and phenolic constituents. Xylose, the main component released in the hemicellulosic hydrolyzates, was maximized by using a 3**(2-0) full factorial design combined with desirability function. At optimum conditions set at 130ºC and 3% (w/v) H_2SO_4, this value was 22.6 g L^{-1} xylose. Three concentrations of activated charcoal (1, 2.5 and 5% w/v) were evaluated to remove certain unwanted byproducts, and it was found that under the highest dosage, 95.27±0.03% of the color was removed with an almost total reduction of furan derivatives, making this liquor an appropriate basis for the development of suitable culture media for lactic acid bacteria. To validate this hypothesis three lactic acid bacteria, namely *Lactobacillus plantarum, Lactobacillus pentosus* and *Lactococcus lactis* were positively tested finding lactic acid yields of 0.89, 0.92 and 0.83 g/L·h respectively.

Keywords: chestnut wastes, prehydrolysis, hemicellulosic hydrolyzates, activated charcoal, detoxification.

1. Introduction

A current concern in Europe's agro-food sector is the search for a productive use of the thousands of tons of crop wastes generated yearly, given that such waste involves significant economic and environmental management costs (Aires et al., 2016). For instance, in 2016 the Mediterranean countries alone produced and processed about 143,256 tons of chestnuts (*Castanea sativa*), the main European producers being Italy (36%), Greece (22%), Portugal (19%) and Spain (11%) ("FAOSTAT," 2018). In the region of Galicia (NW of Spain), the food industry uses about 7,000 tons per year of chestnuts for the production of marron-glacé, chestnut purée and other products (Santos et al., 2017). This industry generates tons of waste, including leaves, prunings and burrs from chestnut trees as well as chesnut shells.

These residues have typically been left in the soil, promoting the growth of insect larvae and consequently leading to crop damage (Vázquez et al., 2012), or they are burned in the field, impacting negatively on the atmosphere and the land, and representing one of the main sources of toxic emissions (some of these similar to dioxins, e.g., CO, NOx, long-chain/aromatic hydrocarbons, polychlorodibenzodioxins) (Morana et al. 2017) and pollutants, if pesticides and heavy metals remain in the composition of the ash (Picchi et al. 2018). Currently, new strategies such as composting are being considered (Ventorino et al. 2016). However, on the same lines as the refining of petroleum, which produces multiple fuels and chemicals, the concept of biorefinery establishes that lignocellulosic biomass can be fractionated into its three main compounds (cellulose, hemicelluloses and lignin) that can then be further converted into a variety of high volume liquid fuels and high value chemicals (Smichi et al. 2018). Therefore, the cell walls of lignocellulosic materials can be degraded into their constituents by hydrolytic processes (acid-catalyzed or hydrothermals), turning them into mixtures of oligomeric and monomeric sugars such as xylose, mannose,

51 galactose, arabinose, hydroxycinnamic and acetic acids from the non-cellulose
52 polysaccharides. That is, lignocellulosic biomass is a source of compounds that can be
53 transformed into high value-added products such as bio oil, biogas, or other bio-based
54 chemicals with a wide array of industrial applications (Arevalo-Gallegos et al. 2017;
55 Bhowmick et al. 2018). During the optimization of the hemicellulosic hydrolysis, the
56 objective is to obtain the highest yield of sugars, but also to minimize the formation of
57 compounds which can be inhibitory of microbial growth, by adjusting parameters such as
58 temperature, acid concentration, liquid-to-solid ratio and reaction time (Brito et al., 2018).

59 Although the tolerance to inhibitory compounds depends on the microorganism used and
60 the operational conditions assayed, a reduction in the concentration of microbial inhibitors
61 might decrease fermentation times and increase the efficiency of sugar use and product
62 formation (Mateo et al., 2013). Detoxification with activated charcoal has been widely
63 reported to remove those phenolic compounds (among others) present in acid hydrolyzates
64 obtained from different materials including chestnut (*Castanea sativa*) shells (Morana et
65 al., 2017), palm press fiber (Brito et al., 2018), potato peels, wheat bran, barley bran
66 (Karasu-yalcin, 2016), olive tree pruning residue (Mateo et al., 2013) and corncob (Gupta
67 et al., 2017).

68 Raw or detoxified hemicellulosic hydrolyzates have been assayed as culture media for
69 several applications, including the production of lactic acid (Alves de Oliveira et al., 2019),
70 bacteriocins (Paz et al. 2017), biosurfactants (Brito et al., 2018), biogas (Santos et al. 2018)
71 and xylitol (Bustos Vázquez et al. 2017), among others. Although many microorganisms
72 have been employed, the use of lactic acid bacteria (LAB) have a high potential because
73 they are safe for human consumption and because they produce various antimicrobial
74 compounds such as organic acids, including lactic acid (da Silva Sabo et al., 2017).
75 Therefore, lactic acid obtained by fermentative processes finds applications not only in the

food industry but also in the chemical, cosmetic, and pharmaceutical sectors, as well as a great potential for the production of biodegradable and biocompatible polylactic polymers that can be employed from packaging to fibers and foams (Portilla Rivera et al., 2015). However, LAB are catalogued as fastidious-growing microorganisms with numerous requirements for growth including amino acids, peptides, vitamins, and nucleic acids (Rodríguez-Pazo et al., 2016).

Chestnut wastes are a source of carbohydrates susceptible to be used in biorefineries. The current study deals with the characterization of four kinds of waste from the industrial processing of chestnuts (*Castanea sativa*), and the subsequent selection of the material with the highest polysaccharide content. Chestnut burrs were fractionated by acid-prehydrolysis and the process optimized through an incomplete factorial design to maximize the amount of xylose released. Finally, in order to formulate suitable culture media, the hemicellulosic hydrolyzates were neutralized and detoxified with charcoal to reduce color and the concentration of inhibitory compounds. The suitability of this culture medium was validated with three lactic acid bacteria: *Lactococcus lactis* subsp. *lactis* CECT 4434, *Lactobacillus pentosus* CECT 4023 and *Lactobacillus plantarum* CECT 221, selected due to their high nutritional requirements.

2. Material and methods

2.1. Chemicals

All chemicals and reagents used in this study were of analytical grade and obtained from Panreac Química SLU (Barcelona, Spain) and Sigma–Aldrich (St. Louis, MO, USA). The solvents employed were of high-performance liquid chromatography (HPLC) grade, and water was ultra-pure. HPLC calibration curves were created for all the standards by injection of different stock concentrations.

2.2. Materials

The study uses four residues obtained from the harvesting and processing of chestnuts, namely leaves, prunings and burrs of the chestnut tree and chestnut shells. All these materials were obtained from local cultivars harvested in September/October 2016 in Galicia, north-west Spain, and supplied by Soutos Sativa S.L., (Monterroso, Lugo, Spain), a local company involved in the cultivation, processing and commercialization of chestnuts. The samples were dried at room temperature before submitting them to grinding, sieving and homogenization to obtain a homogenous material, prior to the storage and conservation at room temperature so as to guarantee stability until use.

2.3. Microorganism and culture media

Lactococcus lactis subsp. *lactis* CECT 4434, *Lactobacillus pentosus* CECT 4023 and *Lactobacillus plantarum* CECT 221 were obtained from the Spanish Collection of Type Cultures (Valencia, Spain) and maintained in cryovials on 30% (v/v) glycerol and growth media at -80 ºC. The strains were grown for 24h on plates using the Man-Rogosa-Sharpe (MRS) medium formulated with 10 g L^{-1} peptone, 8 g L^{-1} beef extract, 4 g L^{-1} yeast extract, 20 g L^{-1} D-glucose, 2 g L^{-1} K_2HPO_4, 2 g L^{-1} di-ammonium hydrogen citrate, 5 g L^{-1} CH_3COONa, 0.2 g L^{-1} $MgSO_4 \cdot 7H_2O$, 0.05 g L^{-1} $MnSO_4 \cdot 2H_2O$, 1 g L^{-1} Tween-80 and 20 g L^{-1} agar. A loop full of a slant culture was transferred to 250 mL Erlenmeyer flasks containing 100 mL of MRS medium without agar and incubated for 24h at 30 ºC and 150 rpm in orbital shaker (Optic Ivymen System, Comecta S.A., distributed by Scharlab, Madrid, Spain).

Cells were recovered by centrifugation (Ortoalresa, Consul 21, EBA 20, Hettich Zentrifugen, Germany) at 3700 × *g* for 15 min and rinsed twice with sterile phosphate buffer saline (PBS) at pH 7.4 (containing 10 mM KH_2PO_4 $K_2HPO_4^{-1}$ and 150 mM NaCl) before inoculation (Bustos et al., 2018).

2.4. Characterization of plant materials

Plant materials were oven-dried (Binder-Model 53 ED, Tuttlingen, Germany) to a constant weight at 105ºC in order to determine the percentage of humidity. The ash content was measured using a muffle furnace (Carbolite ELF 11/6B with 301 controller, Derbyshire, United Kingdom) for 6 h at 575ºC. Nitrogen and carbon percentages were analyzed using a Thermo Finningan Flash Elemental Analyzer 1112 series, San Jose, CA (USA). The composition of plant materials was determined by quantitative acid hydrolysis in two-stages (Paz et al., 2018). Briefly, each material was treated for 1h with 72 wt% sulfuric acid at 30ºC, then sulfuric acid was diluted to 4 wt% and heated at 121ºC for 1 h. The solid residue obtained after hydrolysis was oven-dried at 105ºC and considered as Klason lignin. The analysis of the liquid fraction by High Performance Liquid Chromatography (HPLC) is described below. The quantitative acid hydrolysis liquor was diluted 10 times with 4 wt% sulfuric acid and measured at an absorbance of 205 nm in a UV-Vis Spectrophotometer (Libra S60-Biochrom, Cambridge, U.K.) to determine the acid-soluble lignin. The contents of the extracts were obtained after leaving the material (1-5 g) under reflux for 12-24 hours using ethanol (Ethanol absolute, reagent grade, ACS, ISO, Scharlau, Sentmenat, Barcelona, Spain) as a solvent in a Soxhlet (Behrotest In-Line Extraction Units, Behr Labor-Technik, distributed by Fisher Scientific, Madrid, Spain).

The minerals K, Cu, Fe, Mn, Mg, Ca, Na, Si and Zn were measured in an Atomic Absorption Spectrometer Varian SpectrAA 220 Fast Sequential (Varian Inc., Palo Alto, CA, USA). The metallic elements Cr, Ni, Pb, and Al were determined using an ICP-MS Thermo Elemental X7 (Waltham, Massachusetts, USA). All mineral elements were quantified after acid digestion using 0.4 g of the sample with 8 mL HNO_3 and 3 mL H_2O_2 in a Microwave (CEM, MARSXpress model, Matthews, North Carolina, USA).

All parameters were performed in triplicate and standard deviations reported.

2.5. Hydrolytic treatments

Lignocellulosic material was hydrolyzed with diluted sulfuric acid (prehydrolysis) in an autoclave (Trade Raypa SL, Terrassa, Barcelona) using a liquid/solid ratio of 8 g/g. Aliquots from the reaction media were taken, cooled, filtered with 0.45 μm membranes and analyzed by HPLC using the procedure described below. The effect of time was evaluated with dried chestnut burrs using 3% (w/v) H_2SO_4 and 130°C for 15, 30 and 60 min in 250 mL Pyrex bottles. Hydrolyses were carried out in triplicate and mean values and their standard deviations reported in the corresponding Tables.

2.6. Box–Behnken response surface methodology

A 3**(2-0) full factorial design was planned to optimize the release of carbohydrates using the hydrolysis time previously optimized (30 min). The design contained two independent variables at three levels (−1, 0, 1). The values of these independent variables were: temperature (100, 115, and 130ºC) and H_2SO_4 concentration (1, 3, and 5% w/v). For statistical calculations, the independent variables were coded as x_1 and x_2, respectively, according to the equations:

$$x_1 = (T - 115)/15 \quad \text{(Eq. 1)}$$

and

$$x_2 = ([H_2SO_4] - 3)/2 \quad \text{(Eq. 2)}$$

The dependent variables studied were the concentration of the main components released (g L^{-1}): glucose (y_1), xylose (y_2), arabinose (y_3), acetic acid (y_4), furfural (y_5) and 5-hydroxymethylfurfural (HMF) (y_6).

The design was carried out in one block comprising 12 experimental runs including 9 factorial experiments, and three additional replicates at the center of the experimental domain (0) for the estimation of the pure error. This type of designs allows for the estimation of the significance of the individual parameters and their interactions.

The influence of the independent variables on the dependent variables was assessed using the Statistic software package version 8.0 (Stat Soft, USA). The responses obtained were subjected to analysis of variance (ANOVA). The statistical significance of the independent variables on the responses was determined by evaluating the probability *p*-value and Fisher's test with a 95% confidence level obtained from the ANOVA. Data from the factorial design were subjected to a second-order multiple regression analysis using a least squares regression methodology to obtain parameters of the mathematical model. The interrelationship between dependent variable y_i and operational variables was fitted by a polynomial quadratic equation established through a model including linear, quadratic and interaction terms:

$$y_i = b_0 + b_1x_1 + b_{11}x_1^2 + b_2x_2 + b_{22}x_2^2 + b_{12}x_1x_2 \quad \text{(Eq. 3)}$$

where y_i is the predicted response; x_1 and x_2 are the coded independent variables; b_0 is the model constant; b_1 and b_2 are linear coefficients; b_{11} and b_{22} are quadratic coefficients; and b_{12} are the lineal cross-product coefficients. For each run, predicted values were calculated from the regression equation.

The quality of the polynomial model equation was expressed by determining coefficient R^2, adjusted R^2, and lack of fit. Tridimensional surface plots illustrate the relationship and interaction between coded variables and the responses.

2.7. Optimization of the operational conditions and validation of the model

The profile for predicted values and desirability option from the Statistic software package version 8.0 (Stat Soft, USA) was used for the optimization of the xylose released, as well as for validation of the experimental model.

2.8. Neutralization and detoxification of hemicellulosic hydrolyzates and fermentation conditions

The liquid phase from the acid hydrolysis was neutralized with NaOH to a final pH of 7.0 (Seong et al., 2016). Neutralized hydrolyzates were detoxified with activated powdered charcoal (activated Charcoal for analysis, Panreac Química, Barcelona, Spain) at a mass ratio of hydrolyzate: activated charcoal of 1, 2.5 or 5% (w/v) at a temperature of 30ºC with stirring at 150 rpm (Orbital shaking incubators, WY-100, Comecta S.A., distributed by Scharlab, Madrid, Spain) for 12 h. Liquors were recovered by means of filtration (Bustos Vázquez et al. 2017), diluted with distilled water 1/1 (v/v) and sterilized by autoclave (Trade Raypa SL, Terrassa, Barcelona) at 121 ºC during 15 min.

Fermentations were done in 250 mL Erlenmeyer flasks containing 100 mL of raw or detoxified neutralized hemicellulosic hydrolyzates supplemented with the nutrients of MRS medium except glucose, and placed in orbital shakers at 150 rpm and 30°C

Samples (2 mL) were taken at given fermentation and filtered with 0.22 µm pore size filters. The supernatants were frozen for subsequent analyses.

Fermentations and measurements were done in triplicate, and the means are reported. The global volumetric productivities (Q_P) were calculated for the fermentation times corresponding to the transition from high to low slope of the sigmoidal lactic acid profiles.

2.9. Analytical methods

Glucose, xylose, arabinose and acetic acid were measured through HPLC (Agilent, model 1200, Palo Alto, CA) using a refractive index detector with an Aminex HPX-87H ion exclusion column (Bio Rad 300 × 7.8 mm, 9 µ particles) with a guard column, eluted with 0.003 M of sulfuric acid at a flow rate of 0.6 mL min^{-1} at 50ºC. Five µL of diluted samples were injected, and after this, concentrations were obtained using the corresponding

223 calibration curve. Furfural and HMF were analyzed using a reverse phase HPLC system
224 (Agilent model 1200, Palo Alto, CA, USA) with a UV-diode array detector and a 4.6x150
225 mm Zorbax SB-Aq column (Agilent, Palo Alto, CA, USA) following the elution program
226 described by Paz et al. (2016). The identification of compounds was achieved by
227 combining the spectrum of each molecule with its retention time. Quantification was
228 performed through extrapolating the peak areas using the equation from the corresponding
229 standard curves.
230 Total phenolic content was determined by the Folin-Ciocalteu method (Singleton, V L. and
231 Rossi, 1965). Briefly, 0.5 mL of the sample was mixed with 3.75 mL of distilled water and
232 0.25 mL of Folin reagent previously diluted in distilled water (1:1 v/v). Then, 0.5 mL of
233 sodium carbonate (10% w/v) was added. The mixture was vigorously stirred and incubated
234 for 1h at room temperature. Samples were measured at 765 nm absorbance against a blank.
235 The content of total phenols was calculated in gallic acid equivalents using a calibration
236 curve (0-1 g L^{-1}).
237 Color intensity was analyzed in a supernatant using a UV-Vis Spectrophotometer (Libra
238 S60-Biochrom, Cambridge, U.K.) at an absorbance wavelength of 276 nm. Prior to the
239 measurement, samples were diluted to get a maximum absorbance wavelength value close
240 to 1.0.
241 The percentage of decolorization (D %) was calculated as follows equation:
242 $$D(\%) = \frac{A_{raw} - A_{detoxified}}{A_{raw}} \; x \; 100 \qquad \text{(Eq. 4)}$$
243 Where A_{raw} was the absorbance value of the raw hydrolyzate and $A_{detoxified}$ was the
244 absorbance value after each detoxification treatment.
245 **2.10. Statistical analysis**
246 The data obtained were analyzed with the statistical package SPSS Statistics® (version
247 19.0, SPSS Inc., Chicago, IL, USA), performing T tests for the equality of means (t-

248 Student) where necessary. A value of $p < 0.05$ was considered significant. Each value in
249 the graphs was expressed as mean ± Standard Deviation (SD) of three independent
250 experiments, conducted in triplicates.
251 On the hand, data tables 1 and 2 were analyzed with Statgraphics Centurion XVI (Version
252 16.1.11). The method currently being used to discriminate among the means is Tukey's
253 honestly significant difference (HSD) procedure. With this method, there is a 5,0 % risk of
254 calling one or more pairs significantly different when their actual difference equals 0.
255

256 **3. Results and discussion**

257 **3.1. Chemical composition of materials**

258 **Table 1** shows the compositional analysis of the selected chestnut wastes (leaves, prunings
259 and burrs of chestnut trees, and chestnut shells). The elemental analysis (content in C and
260 N) reveals that the carbon content is similar among samples, ranging between 42.8-47.3%.
261 However, it is worth noting that there is a higher nitrogen content for the prunings (1.4 ±
262 0.0), doubling the value attained for the other materials.
263 Regarding the mineral content of the samples, the amount of Zn found in chestnut prunings
264 (83.9 ± 1.6 mg kg^{-1}) is notable, being 10 times higher than in the other samples. Something
265 similar happens with Cu, where the content observed in prunings (9.0 ± 0.2 mg kg^{-1}) is
266 clearly higher. On the contrary, leaves showed higher levels of Na, K, Al and Mn.
267 Meanwhile, Ca, Mg and Fe were found in different proportions without being of particular
268 note in any one material. The remaining minerals (Si, Cr, Ni and Pb) were not quantified,
269 with the exception of 1.4 ± 0.1 mg kg^{-1} of Ni in prunings.
270 Table 1 also shows their polymeric content: percentages of glucan, xylan and arabinan.
271 Therefore, two types of material can be clearly differentiated. Leaves and shells are
272 characterized by their low percentages of glucan (16.54 ± 0.21 and 14.87 ± 0.16 %

273 respectively), xylan (11.68 ± 0.14 and 10.04 ± 0.16 % respectively) and arabinan (2.97 ±
274 0.10 and 2.91 ± 0.10 % respectively), without significant differences between them ($p > 0.05$), and were discarded due to being of little use for the production of sugars solutions.
276 In addition, these wastes showed a higher presence of Klason lignin (37.54 ± 0.37 and
277 44.31 ± 1.03%, respectively), which might also limit the generation of culture media,
278 independently of whether the chemical composition of lignin (its compositional
279 monomers) might be a more significant determinant than its amount for lignocellulose
280 recalcitrance during the pretreatment (Gall et al. 2017; Kim et al. 2017). On the other hand,
281 burrs and prunings show higher polysaccharide content, with significant different ($p < 0.05$) regarding the other materials, and relatively low lignin values. In particular, the
283 higher content of glucan (34.39 ± 2.1%) and xylan (21.34 ± 1.3%) found in burrs, along
284 with the lower amount of Klason lignin (22.61 ± 1.1%), makes burr wastes the most
285 promising for carrying out the subsequent stages of acid hydrolysis.
286 Few studies in the literature provide information on the chemical composition of these
287 materials. For instance, Vázquez et al. (2008) observed lower values of glucan (19.23%)
288 and higher content of acid-insoluble lignin (29.15%) during the characterization of
289 chestnut (*Castanea sativa*) shells. The compositional differences can be ascribed to the
290 inherent properties of the lignocellulosic materials, such as the origin of the material, the
291 geographical location and growth conditions, as well as the type of tissue analyzed.

292 **3.2. Influence of time on the chemical processing of chestnut burrs**

293 When a raw material is subjected to a mild hydrolysis with diluted acids (prehydrolysis),
294 what is obtained is a solution rich in hemicellulosic sugars, mainly xylose, and a solid
295 residue containing the untreated cellulose and lignin. The optimization of this treatment
296 usually adjusts process parameters such as temperature, acid concentration, liquid-to-solid
297 ratio and the reaction time, which must be changed according to the target biomass to

298 obtain the maximum yield of sugars and a minimum formation of toxic compounds (Brito
299 et al. 2018). Therefore, depending on the duration of the hydrolysis, some acetic acid
300 liberated from the acetyl groups of the material may also appear, as well as smaller
301 amounts of furfural and HMF generated by the dehydration of pentoses and hexoses,
302 respectively. These compounds are toxic inhibitors on microbial metabolism (Brito et al.
303 2018). Considering that one of the parameters to set is the time of hydrolysis, Table 2
304 shows the data obtained after the treatments carried out with 3% (w/v) H_2SO_4 at 15, 30 and
305 60 minutes. As can be seen, prehydrolysis results in the solubilization of sugars, with the
306 highest values, 23.48 ± 0.16 g L^{-1} xylose, 6.69 ± 0.02 g L^{-1} glucose and 3.31 ± 0.05 g L^{-1}
307 arabinose, being attained at an intermediate treatment time (30 min). In addition, when
308 reaction times increased at 60 min, a slight increase, with significant difference ($p < 0.05$)
309 is observed in the amount of furfural (0.64 ± 0.02 g L^{-1}) and HMF (0.17 ± 0.01 g L^{-1}).
310 Hence, the time of 30 minutes was chosen for the experimental design. This value is
311 intermediate of those reported in literature depending on the material studied. For instance,
312 Bustos et al. (2004) reported best operational conditions using 3% H_2SO_4 during only 15
313 min during the production of fermentable media from vine-trimming wastes; meanwhile
314 harsher conditions were necessary for acid pre-treatment of palm press fiber with a view to
315 the release of reducing sugars: 5.33% (w/v) H_2SO_4 and a hydrolysis time of 61.49 min
316 (Brito et al. 2018).

317 **3.3. Box–Behnken response surface methodology**

318 Acid hydrolysis also depends on other parameters, such as temperature and percentage of
319 acid. Because the study of the individual effects of each condition requires a large amount
320 of experimental work, a factorial design was carried out to simplify the experimentation
321 (Rivera et al., 2007). Several research groups have used phenomenological models based

on experimental designs to study the chemical processing and/or bioconversion of lignocellulosic materials (Bustos Vázquez et al., 2017; Salgado et al., 2015).

Table 3 shows the set of experimental conditions assayed (expressed in terms of coded variables) as well as the experimental data obtained for dependent variables y_1 to y_6. The sequence for the experimental work was randomly established to limit the influence of systematic errors. Experiments 10–12 are additional replications in the central point of the design (experiment 5) to measure the experimental error.

The quality of the developed models was evaluated based on the coefficient of determination (R^2) and the adjusted coefficient of determination (R^2 adjust). Table 4 shows this information. The worst results were achieved with variable y_2 (xylose), in which the coefficients were 0.93 and 0.88 respectively, indicating that 93% of the xylose released was attributed to the experimental variables studied, and the model could only fail to explain 7%. Table 4 also provides the ANOVA analysis that we used to determine the significance of the developed quadratic model by the lack of fit test. Lack of fit is a diagnostic test that compares the pure error based on the replicate measurements and shows the adequacy of the model. A *p*-value higher than 0.05 indicates that lack of fit is insignificant and hence determines that the quadratic model was valid for the study in question, whereas significant results means that the variation of the replicates in relation to their mean values is less than the variation of the design points about their predicted values. The drawback of this model is that it does not provide a good prediction when the runs replicate well and their variance is small. This was seen with HMF, in the pure error here of 0.00. In this case, the accuracy of the model was validated based on R^2 value (0.98) (Nasirizadeh et al. 2012; Vera Candioti et al. 2014). Finally, Table 4 also provides probability F-test and *p*-values to estimate the significance of each term. Large F-values

show that the variation can be explained by the developed regression equation. On the other hand, *p*-values lower than 0.05 indicate the statistically significant terms.

A Pareto chart was made (Figure 1) to visualize the contribution of each standardized effect on the release of compounds. In these figures, each bar is proportional to the estimated effect, and the vertical line (*p*-value = 0.05) is used to evaluate those effects which are statistically significant at a 95% confidence level. Six mathematical models were obtained to predict the different compounds released (y_i), in which those terms that are not statistically significant for the treatment ($p < 0.05$) were excluded for the regression equations, and presented as:

$$y_1 = 2.197184 + 1.440508x_1 + 0.523003x_2 - 0.166122x_1^2 + 0.225855x_2^2 + 0.372181x_1x_2 \quad \text{(Eq. 5)}$$

$$y_2 = 13.47660 + 7.63710x_1 + 3.79282x_2 \quad \text{(Eq. 6)}$$

$$y_3 = 3.507738 + 0.246743x_1 - 0.104474x_2 + 0.092454x_2^2 - 0.385898x_1x_2 \quad \text{(Eq. 7)}$$

$$y_4 = 3.642401 + 1.164617x_1 + 0.856982x_2 + 0.351834x_2^2 - 0.528887x_1x_2 \quad \text{(Eq. 8)}$$

$$y_5 = 0.202157 + 0.219017x_1 + 0.139961x_2 - 0.058166x_1^2 + 0.142579x_1x_2 \quad \text{(Eq. 9)}$$

$$y_6 = 0.082680 + 0.060322x_1 + 0.017620x_2 - 0.011711x_1^2 - 0.013790x_2^2 \quad \text{(Eq. 10)}$$

The positive coefficients of both linear independent variables (with the exception of Eq.6) indicate that high temperatures (x_1) and percentages of acid (x_2) within the studied range favored the release of all the compounds. The negative quadratic effect observed in temperature (x_1^2) in Eq.4 can be interpreted as, beyond the maximum point, the dehydration of glucose is promoted by sulfuric acid to produce 5-hydroxymethylfurfural (Brito et al. 2018).

Figure 2 shows 3D surface plots of the predicted dependence of dependent variables (y_i) on the operational variables (T and % H_2SO_4) generated on the base of the second-order polynomial equation. As a general trend, the curvatures of these plots show the effect of interaction, and the remarkable increases with the harsher conditions (defined by high

values of temperature and/or % H_2SO_4). Furthermore, the curvature of temperature (x_1) is less pronounced, and in particular temperature shows no influence under the harder concentrations of acid. Additionally, under lower concentrations of acids, temperature was not influential in variables y_1 (glucose) and y_5 (furfural), hardly influential in variable y_6 (HMF), and indeed was detrimental in variable y_3 (arabinose). Hence, the effect of sulfuric acid was more relevant in general.

3.4. Optimization of the operational condition y_2 (xylose concentration) and validation of the model

Under the severest conditions considered (130ºC and 5% H_2SO_4), the model predicted the released of up to 24.9 g L^{-1} of xylose. However, when using the desirability option from the Statistic software package, the value predicted (see Figure 3) was y_2 = 22.60 g L^{-1} of xylose, this being achieved when x_1 = 1 and x_2 = 0.5, corresponding to 130ºC and 3% (w/v) H_2SO_4, respectively.

In order to validate the model, a new experience was carried out in triplicate under the optimal conditions obtained when applying the desirability option, and the results obtained were: 6.91 ± 0.11 g L^{-1} glucose, 22.31 ± 0.12 g L^{-1} xylose, 3.32 ± 0.21 g L^{-1} arabinose, 5.02 ± 0.31 g L^{-1} acetic acid, 0.70 ± 0.01 g L^{-1} furfural and 0.20 ± 0.01 g L^{-1} HMF.

As can be seen, the value obtained for xylose (22.31 ± 0.12 g L^{-1}) is similar to the 22.60 g L^{-1} predicted by the model, and thus it can be considered an appropriate model.

3.5. Neutralization and detoxification of hemicellulosic hydrolyzates

Acid hydrolysis releases not only the monomeric sugars susceptible to be fermented (glucose, xylose and arabinose), but also several microbial inhibitors, which can cause inhibition of microbial metabolism and reduce cell growth and product yield, including low-molecular-weight phenolic compounds, furan derivatives such as furfural, HMF, aliphatic acids such as formic acid, levulinic acid, and acetic acid, or even minerals/metals

contained in the lignocellulosic materials or resulting from the corrosion of the hydrolysis equipment (Bustos Vázquez et al. 2017; Lee et al. 2011). In this study we have focused on three types of inhibitors: aliphatic acids (acetic acid), furan derivatives (furfural and HMF) and phenolic compounds.

In our case, the acid hemicellulosic hydrolyzate obtained under optimized conditions exhibited a dark color and the following composition: aliphatic acids (5.00 ± 0.26 g L^{-1} acetic acid), furans (0.65 ± 0.00 g L^{-1} furfural and 0.19 ± 0.00 g L^{-1} HMF) and phenolic compounds (2.38 g L^{-1} equivalent to gallic acid), making the hydrolyzate unsuitable for microbial growth (Behera et al., 2014; Chandel et al., 2013; Palmqvist, 2000). Acetic acid formation is mainly due to the degradation of the hemicellulose glucuronoxylan, where acetyl groups (at carbon 2 or 3 of the glucuronoxylan backbone) are cleaved (Lee et al. 2011). When acetic acid and formic acid (a degradation product of HMF) enter in the cell in the undissociated form, they become dissociated in the protoplasm because of its pH, leading to a decrease in the intracellular pH that can generate cell death (Mateo et al., 2013). Phenolic compounds cause the loss of integrity of biological membranes, thereby affecting their ability to serve as selective barriers and enzyme matrices (Brito et al. 2018; Mateo et al. 2013). The furans derivatives furfural and HMF are formed by the hydrolysis of pentoses and hexoses, respectively. *In vitro* evaluations have shown that furans directly inhibit alcohol dehydrogenase (ADH), pyruvate dehydrogenase (PDH) and aldehyde dehydrogenase (ALDH) and cause acetaldehyde accumulation which subsequently prolongs the lag-phase of fermenting microorganisms (Gupta et al., 2017).

Consequently, three dosages of activated charcoal (1, 2.5 and 5% w/v) were assayed to detoxify the neutralized hydrolyzate. Activated charcoal has been assayed widely in different hemicellulosic liquors. For instance, Brito et al. (2018) reduced the content of total phenolic compounds, furfural and HMF in palm press fiber hemicellulosic

hydrolyzates using 5% (w/v) activated charcoal from 0.66 ± 0.03 g L^{-1}, 489.50 mg L^{-1} and 46.14 mg L^{-1} to 0.06 ± 0.01 g L^{-1}, 3.37 mg L^{-1} and undetected, respectively. Lee et al. (2011) using 2.5% activated carbon in autohydrolysis prehydrolyzate from mixed hardwood chips, were able to remove 42% of formic acid, 14% of acetic acid, 96% of HMF and 93% of the furfural, although they also removed 8.9% of sugars. Mateo et al. (2013) also decreased inhibitors from olive tree pruning residue hydrolyzates (removing 46% of acetic acid, 81% of phenolic compounds and 98% of total furans) with 2% charcoal. Meanwhile Morana et al. (2017), with 5% (w/v) activated charcoal and repeated adsorption-desorption processes, enabled the recovery of 70.3% (w/w) of phenolic compounds in chestnut shell hydrolyzates, whilst simultaneously retaining the soluble sugars in the detoxified hydrolyzate.

Figure 4 shows the color removal at different activated charcoal dosages. It can be observed that, independently of the amount of charcoal assayed, a high color removal rate was reached up to 2 h, and then equilibrium was reached. This tendency can be interpreted in light of the high initial number of sites in activated charcoal, hence the greater driving force for the mass transfer and consequently the phenolic compounds reacted easily at adsorption sites. After 2 h, the number of free sites decreased and the non-adsorbate molecules were assembled at the surface, thus limiting the capacity of adsorption (Gupta et al., 2017).

On the other hand, Table 5 shows the amounts of monosaccharides released, as well as those toxic compounds present in the raw hydrolyzate and the liquors obtained after detoxification with activated charcoal under different dosages. A clear increase can be observed in the amount of substances removed with the increase of charcoal, with the exception of acetic acid, which remained constant. Brito et al. (2018) also observed an increment of acetic acid from 12.02 to 16.65 g L^{-1} after the treatment with 5% (w/v)

448 activated charcoal. On the positive side, the concentration of sugars was only slightly
449 reduced with the increase of charcoal assayed. Conversely, Brito et al. (2018) observed
450 that treatment with activated charcoal resulted in an increase in the concentration of the
451 reducing sugars from 83.1 to 94.9 g L^{-1} in the hydrolyzate. A similar increase was also
452 observed by Díaz et al. (2009) with 5% (w/v) activated charcoal, the authors here
453 concluding that the increase in sugar concentration occurred as a result of the evaporation
454 of water during the treatment, which required heating at 50ºC for 60 min. However, this
455 cannot be applied to our results since the process was carried out at room temperature.

456 The most important finding was that furan derivatives and phenolic compounds underwent
457 the highest percentages of elimination. Thus, using 1% charcoal, the amounts of phenolic
458 compounds decreased from 2.38±0.00 g L^{-1} in raw hydrolyzates to 0.27 ± 0.00 g L^{-1} and up
459 to 0.02 ± 0.00 g L^{-1} with 5%, with percentages of color removal of 51.30 ± 0.28 and
460 95.27±0.03 %, respectively. Similarly, furfural was completely removed with 2.5%
461 charcoal, and HMF was reduced from 0.06±0.00 g L^{-1} in raw hydrolyzates to 0.02±0.00 g
462 L^{-1} in hydrolyzates detoxified at the highest level (5%).

463 **3.6. Fermentation of neutralized hemicellulosic hydrolyzates**

464 In order to assay the fermentability of hemicellulosic hydrolyzates, three fastidious-
465 growing microorganisms *Lactococcus lactis* subsp. *lactis* CECT 4434, *Lactobacillus*
466 *pentosus* CECT 4023 and *Lactobacillus plantarum* CECT 221 were cultivated separately
467 for 36h in raw or detoxified neutralized hemicellulosic hydrolyzates. In all cases, a
468 prolonged lag period was observed (data not shown). Consequently, hydrolyzates were
469 diluted with distilled water in the proportion 1/1 (v/v) in order to reduce the toxic effect of
470 inhibitory compounds. Therefore, a new set of experiments was carried out using diluted
471 hydrolyzates. In this case, it was observed the complete absence of sugars (glucose, xylose
472 and arabinose) consumption, and consequently the negligible production of lactic acid and

acetic acid when the strains were grown in raw diluted hemicellulosic hydrolyzates (left column of **Figure 5**). Conversely, all the strains produced different amounts of lactic acid when detoxified diluted acid hydrolyzates were assayed. **Table 6** shows the stoichiometric parameters, productivities and yields for bioconversion assays. The best results were obtained with the strain *L. plantarum*, since a regular increase in lactic acid was quantified till 12h, remaining almost constant thereafter. The maximum lactic acid production was 6.85 g/L, corresponding to a global volumetric productivity of lactic acid (Q_P) of 0.51 g/L·h; a sugars consumption rate (Q_S) of 0.58 g/L·h; and a product yield ($Y_{P/S}$) of 0.89 g/g. *L. pentosus* showed a similar tendency, although the growth was slightly slower, being necessary 20h to reach a highest lactic acid concentration of 6.56 g/L (Q_P = 0.29 g/L·h; Q_S = 0.32 g/L·h and $Y_{P/S}$ = 0.92 g/g). Finally, although *L. lactis* experienced the lowest production, 4.15 g/L lactic acid was obtained after 20h (Q_P = 0.18 g/L·h; Q_S = 0.21 g/L·h and $Y_{P/S}$ = 0.83 g/g). On the other hand, acetic acid, the main by-product of fermentation hardly increased in all experiments. The lactic acid yields superior to 0.83 g/g calculated with the three strains confirm the suitability of detoxified neutralized hemicellulosic hydrolyzate of chestnut burrs as culture broths to carry out fermentative processes.

Conclusions

Chestnut wastes are produced in large amounts worldwide. However, these agroindustrial by-products are undervalued. Due to their lignocellulosic character, they could be used as an economic feedstock for biorefinery processes. The higher content of glucan and xylan found in chestnut burrs, along with the lower amount of Klason lignin, makes this waste the most promising for carrying out the subsequent stages of acid hydrolysis. Hydrolysis catalyzed by dilute sulfuric acid (prehydrolysis) is a suitable technology to recover hemicellulosic sugars, particularly xylose. Intermediate treatment time (30 min) resulted in the highest amounts of sugars released. Operating under selected operational conditions

(130ºC and 3% (w/v) H_2SO_4), high amounts of xylose can be produced, being sulfuric acid more relevant than temperature. However, some inhibitory compounds were also present in the hemicellulosic liquor, including aliphatic acids, furans, and phenolic compounds. Therefore, detoxification with 5% charcoal led to almost complete removal of color and phenolic compounds, making this hydrolyzate a good candidate for the production of culture media suitable for microbial growth under a wide range of microorganisms. This hypothesis was corroborated by growing successfully three lactic acid bacteria in spite of their high requirements to be fermented.

Acknowledgments

The development of this project is financed by the Galician Innovation Agency (Project: Valorización de residuos agroindustriales para la obtención de bioproductos de alto valor añadido "Innobiorresiduos") and co-financed by 80% by the European Regional Development Fund under the Feder Galicia 2014-2020 operational program (OT 1. "Promote technological development, innovation and quality research").

Declarations of interest: none

4. Bibliografía

Aires, A., Carvalho, R., José, M., 2016. Valorization of solid wastes from chestnut industry processing : Extraction and optimization of polyphenols , tannins and ellagitannins and its potential for adhesives , cosmetic and pharmaceutical industry. Waste Manag. 48, 457–464. https://doi.org/10.1016/j.wasman.2015.11.019

Alves de Oliveira, R., Komesu, A., Vaz Rossell, C.E., Wolf Maciel, M.R., Maciel Filho, R., 2019. Concentrating second-generation lactic acid from sugarcane bagasse via hybrid short path evaporation: Operational challenges. Sep. Purif. Technol. 209, 26–31. https://doi.org/10.1016/j.seppur.2018.07.012

Arevalo-gallegos, A., Ahmad, Z., Asgher, M., Parra-saldivar, R., Iqbal, H.M.N., 2017. International Journal of Biological Macromolecules Lignocellulose : A sustainable material to produce value-added products with a zero waste approach — A review. Int. J. Biol. Macromol. 99, 308–318. https://doi.org/10.1016/j.ijbiomac.2017.02.097

Behera, S., Arora, R., Nandhagopal, N., Kumar, S., 2014. Importance of chemical pretreatment for bioconversion of lignocellulosic biomass. Renew. Sustain. Energy Rev. 36, 91–106. https://doi.org/10.1016/j.rser.2014.04.047

Bhowmick, G. De, Sarmah, A.K., Sen, R., 2018. Bioresource Technology Lignocellulosic biore fi nery as a model for sustainable development of biofuels and value added products. Bioresour. Technol. 247, 1144–1154. https://doi.org/10.1016/j.biortech.2017.09.163

Brito, P.L., de Azevedo Ferreira, C.M., Silva, A.F.F., Pantoja, L. de A., Nelson, D.L., dos Santos, A.S., 2018. Hydrolysis, Detoxification and Alcoholic Fermentation of Hemicellulose Fraction from Palm Press Fiber. Waste and Biomass Valorization 9, 957–968. https://doi.org/10.1007/s12649-017-9882-4

Bustos, G., Arcos, U., Vecino, X., Cruz, J.M., Moldes, A.B., 2018. Recycled Lactobacillus pentosus biomass can regenerate biosurfactants after various fermentative and extractive cycles. Biochem. Eng. J. 132, 191–195. https://doi.org/10.1016/j.bej.2018.01.021

Bustos Vázquez, G., Pérez-Rodríguez, N., Salgado, J.M., Oliveira, R.P.D.S., Domínguez, J.M., 2017. Optimization of Salts Supplementation on Xylitol Production by Debaryomyces hansenii Using a Synthetic Medium or Corncob Hemicellulosic Hydrolyzates and Further Scaled Up. Ind. Eng. Chem. Res. 56, 6579–6589. https://doi.org/10.1021/acs.iecr.7b01120

Chandel, A.K., Silvério, S., Singh, O. V, 2013. Detoxification of Lignocellulose Hydrolysates : Biochemical and Metabolic Engineering Toward White Biotechnology 388–401. https://doi.org/10.1007/s12155-012-9241-z

da Silva Sabo, S., Pérez-Rodríguez, N., Domínguez, J.M., de Souza Oliveira, R.P., 2017. Inhibitory substances production by Lactobacillus plantarum ST16Pa cultured in hydrolyzed cheese whey supplemented with soybean flour and their antimicrobial efficiency as biopreservatives on fresh chicken meat. Food Res. Int. 99, 762–769. https://doi.org/10.1016/j.foodres.2017.05.026

Díaz, M.J., Ruiz, E., Romero, I., Cara, C., Moya, M., Castro, E., 2009. Inhibition of Pichia stipitis fermentation of hydrolysates from olive tree cuttings. World J. Microbiol. Biotechnol. 25, 891–899. https://doi.org/10.1007/s11274-009-9966-9

FAOSTAT. URL http://www.fao.org/faostat/en/#data (accessed 5.27.18).

Gupta, R., Hemansi, Gautam, S., Shukla, R., Kuhad, R.C., 2017. Study of charcoal detoxification of acid hydrolysate from corncob and its fermentation to xylitol. J. Environ. Chem. Eng. 5, 4573–4582. https://doi.org/10.1016/j.jece.2017.07.073

Karasu-yalcin, K.E.S., 2016. Evaluation of some lignocellulosic byproducts of food

564 industry for microbial xylitol production by Candida tropicalis. 3 Biotech 6, 1–7.
565 https://doi.org/10.1007/s13205-016-0521-8
566 Mateo, S., Conceic, I., Sánchez, S., Moya, A.J., 2013. Detoxification of hemicellulosic
567 hydrolyzate from olive tree pruning residue 49, 196–203.
568 https://doi.org/10.1016/j.indcrop.2013.04.046
569 Morana, A., Squillaci, G., Paixão, S.M., Alves, L., La Cara, F., Moura, P., 2017.
570 Development of an energy biorefinery model for chestnut (Castanea sativa Mill.)
571 shells. Energies 10, 1–14. https://doi.org/10.3390/en10101504
572 Myoung, J., Venditti, R.A., Jameel, H., Kenealy, W.R., 2010. Detoxification of woody
573 hydrolyzates with activated carbon for bioconversion to ethanol by the thermophilic
574 anaerobic bacterium Thermoanaerobacterium saccharolyticum. Biomass and
575 Bioenergy 35, 626–636. https://doi.org/10.1016/j.biombioe.2010.10.021
576 Nasirizadeh, N., Dehghanizadeh, H., Yazdanshenas, M.E., Moghadam, M.R., Karimi, A.,
577 2012. Optimization of wool dyeing with rutin as natural dye by central composite
578 design method. Ind. Crops Prod. 40, 361–366.
579 https://doi.org/10.1016/j.indcrop.2012.03.035
580 Palmqvist, E., 2000. Fermentation of lignocellulosic hydrolysates . II : inhibitors and
581 mechanisms of inhibition 74, 25–33.
582 Paz, A., Carballo, J., Pérez, M.J., Domínguez, J.M., 2016. Bacillus aryabhattai BA03: a
583 novel approach to the production of natural value-added compounds. World J.
584 Microbiol. Biotechnol. 32. https://doi.org/10.1007/s11274-016-2113-5
585 Paz, A., da Silva Sabo, S., Vallejo, M., Marguet, E., Pinheiro de Souza Oliveira, R.,
586 Domínguez, J.M., 2018. Using brewer's spent grain to formulate culture media for the
587 production of bacteriocins using Patagonian strains. Lwt 96, 166–174.
588 https://doi.org/10.1016/j.lwt.2018.05.027
589 Picchi, G., Lombardini, C., Pari, L., Spinelli, R., 2018. Physical and chemical
590 characteristics of renewable fuel obtained from pruning residues. J. Clean. Prod. 171,
591 457–463. https://doi.org/10.1016/j.jclepro.2017.10.025
592 Portilla Rivera, O.M., Arzate Martínez, G., Jarquín Enríquez, L., Vázquez Landaverde,
593 P.A., Domínguez González, J.M., 2015. Lactic Acid and Biosurfactants Production
594 from Residual Cellulose Films. Appl. Biochem. Biotechnol. 177, 1099–1114.
595 https://doi.org/10.1007/s12010-015-1799-4
596 Rivera, O.M.P., Moldes, A.B., Torrado, A.M., Domínguez, J.M., 2007. Lactic acid and
597 biosurfactants production from hydrolyzed distilled grape marc. Process Biochem. 42,
598 1010–1020. https://doi.org/10.1016/j.procbio.2007.03.011
599 Rodríguez-Pazo, N., Da Silva Sabo, S., Salgado-Seara, J.M., Arni, S. Al, De Souza
600 Oliveira, R.P., Domínguez, J.M., 2016. Optimisation of cheese whey enzymatic
601 hydrolysis and further continuous production of antimicrobial extracts by
602 Lactobacillus plantarum CECT-221. J. Dairy Res. 83, 402–411.
603 https://doi.org/10.1017/S0022029916000352
604 Salgado, J.M., Abrunhosa, L., Venâncio, A., Domínguez, J.M., Belo, I., 2015. Enhancing
605 the Bioconversion of Winery and Olive Mill Waste Mixtures into Lignocellulolytic
606 Enzymes and Animal Feed by Aspergillus uvarum Using a Packed-Bed Bioreactor. J.
607 Agric. Food Chem. 63, 9306–9314. https://doi.org/10.1021/acs.jafc.5b02131
608 Santos, J., Antorrena, G., Freire, M.S., Pizzi, A., González-Álvarez, J., 2017.
609 Environmentally friendly wood adhesives based on chestnut (Castanea sativa) shell
610 tannins. Eur. J. Wood Wood Prod. 75, 89–100. https://doi.org/10.1007/s00107-016-
611 1054-x
612 Seong, H.A., Lee, J.S., Yoon, S.Y., Song, W.Y., Shin, S.J., 2016. Fermentation
613 characteristics of acid hydrolysates by different neutralizing agents. Int. J. Hydrogen

Energy 41, 16365–16372. https://doi.org/10.1016/j.ijhydene.2016.05.003
Singleton, V L.; Rossi Jr, J.A., 1965. Colorimetry of Total Phenolics with Phosphomolybdic-Phosphotungstic Acid Reagents. Am. J. Enol. Vitic. 16, 144–158. https://doi.org/10.12691/ijebb-2-1-5
Smichi, N., Messaoudi, Y., Gargouri, M., 2018. Lignocellulosic Biomass Fractionation : Production of Ethanol , Lignin and Carbon Source for Fungal Culture. Waste and Biomass Valorization 9, 947–956. https://doi.org/10.1007/s12649-017-9859-3
Vázquez, G., Fernández-Agulló, A., Gómez-Castro, C., Freire, M.S., Antorrena, G., González-Álvarez, J., 2012. Response surface optimization of antioxidants extraction from chestnut (Castanea sativa) bur. Ind. Crops Prod. 35, 126–134. https://doi.org/10.1016/j.indcrop.2011.06.022
Vázquez, G., Fontenla, E., Santos, J., Freire, M.S., González-Álvarez, J., Antorrena, G., 2008. Antioxidant activity and phenolic content of chestnut (Castanea sativa) shell and eucalyptus (Eucalyptus globulus) bark extracts. Ind. Crops Prod. 28, 279–285. https://doi.org/10.1016/j.indcrop.2008.03.003
Ventorino, V., Parillo, R., Testa, A., Viscardi, S., Espresso, F., Pepe, O., 2016. Chestnut green waste composting for sustainable forest management : Microbiota dynamics and impact on plant disease control. J. Environ. Manage. 166, 168–177. https://doi.org/10.1016/j.jenvman.2015.10.018
Vera Candioti, L., De Zan, M.M., Cámara, M.S., Goicoechea, H.C., 2014. Experimental design and multiple response optimization. Using the desirability function in analytical methods development. Talanta 124, 123–138. https://doi.org/10.1016/j.talanta.2014.01.034

654 **Table 1.** Characterization of raw materials.

	Chestnut leaves	**Chestnut burrs**	**Chestnut pruning**	**Chestnut shells**
C (%)	47.3 ± 0.2	42.8 ± 0.2	45.0 ± 0.1	46.6 ± 0.5
N (%)	0.6 ± 0.0	0.6 ± 0.0	1.4 ± 0.0	0.7 ± 0.0
Ca (g kg^{-1})	5.7 ± 0.4	1.1 ± 0.1	11.4 ± 1.1	1.3 ± 0.0
Mg (g kg^{-1})	2.7 ± 0.1	0.9 ± 0.0	3.5 ± 0.4	1.0 ± 0.1
Na (mg kg^{-1})	135.0 ± 2.8	29.7 ± 0.4	49.1 ± 2.3	47.4 ± 5.1
K (mg kg^{-1})	148.5 ± 3.5	32.7 ± 0.6	50.4 ± 3.3	48.9 ± 5.4
Al (mg kg^{-1})	434.7 ± 17.7	<300	<300	<300
Si (mg kg^{-1})	<300	<300	<300	<300
Zn (mg kg^{-1})	8.2 ± 0.1	5.8 ± 0.0	83.9 ± 1.6	6.8 ± 0.0
Fe (mg kg^{-1})	55.0 ± 0.4	20.7 ± 0.2	42.5 ± 1.2	11.4 ± 0.1
Mn (mg kg^{-1})	1737.8 ±24.9	184.9 ± 1.1	539.2 ± 11.1	122.4 ± 4.5
Cr (mg kg^{-1})	<1 (0.8)	<1	<1	<1
Ni (mg kg^{-1})	<1 (0.8)	<1 (0.8)	1.4 ± 0.1	<1
Cu (mg kg^{-1})	2.4 ± 0.0	2.4 ± 0.0	9.0 ± 0.2	2.9 ± 0.0
Pb (mg kg^{-1})	<1	<1	<1	<1
Humidity (%)	9.16 ± 0.04^{a}	11.24 ± 0.00^{b}	7.73 ± 0.00^{c}	10.37 ± 0.00^{d}
Ash (%)	2.82 ± 0.06^{a}	0.96 ± 0.03^{b}	4.08 ± 0.22^{c}	0.58 ± 0.10^{b}
Extracts (%)	8.98 ± 0.62^{a}	3.29 ± 0.08^{b}	6.68 ± 0.29^{c}	5.34 ± 0.40^{c}
ASL (%)	6.45 ± 0.28^{a}	$6.88 \pm 0.01^{a,b}$	$6.03 \pm 0.07^{a,c}$	3.90 ± 0.06^{d}
Klason lignin (%)	37.54 ± 0.37^{a}	22.62 ± 1.12^{b}	23.24 ± 0.12^{c}	44.31 ± 1.03^{d}
Glucan (%)	16.54 ± 0.21^{a}	34.39 ± 2.07^{b}	30.72 ± 0.20^{b}	14.87 ± 0.16^{a}
Xylan (%)	11.68 ± 0.14^{a}	21.35 ± 1.30^{b}	17.03 ± 0.13^{c}	10.04 ± 0.16^{a}
Arabinan (%)	2.97 ± 0.10^{a}	$3.05 \pm 0.01^{a,b}$	$2.52 \pm 0.11^{a,c}$	2.91 ± 0.10^{a}
Acetyl groups (%)	3.09 ± 0.17^{a}	$5.45 \pm 0.10^{a,b}$	$4.57 \pm 0.05^{a,c}$	3.04 ± 0.12^{a}

655 ASL: Acid soluble lignin. Same letters show no significant difference ($p > 0.05$).

656

Table 2. Compounds released (expressed in g L^{-1}) during the prehydrolysis stage carried out using 3% (w/v) H_2SO_4 at different times.

	15 min	**30 min**	**60 min**
Glucose	3.57 ± 0.03^{a}	4.25 ± 0.01^{b}	4.74 ± 0.11^{c}
Xylose	22.15 ± 0.13^{a}	23.48 ± 0.16^{b}	22.60 ± 0.13^{a}
Arabinose	3.30 ± 0.03^{a}	3.31 ± 0.05^{a}	3.02 ± 0.11^{a}
Acetic acid	5.36 ± 0.05^{a}	5.35 ± 0.10^{a}	5.50 ± 0.08^{a}
Furfural	0.43 ± 0.01^{a}	0.51 ± 0.01^{b}	0.64 ± 0.02^{c}
HMF	0.11 ± 0.01^{a}	0.15 ± 0.00^{b}	0.17 ± 0.01^{c}

HMF: hydroxymethylfurfural. Same letters show no significant difference ($p > 0.05$).

675 **Table 3.** Operational conditions considered in the hydrolysis of chestnut burrs, expressed in
676 terms of the coded independent variables x_1 (temperature) and x_2 (H_2SO_4 concentration) and
677 experimental results achieved after 30 minutes of hydrolysis for the dependent variables y_1
678 (glucose concentration, g L^{-1}), y_2 (xylose concentration, g L^{-1}), y_3 (arabinose concentration, g
679 L^{-1}), y_4 (AcH concentration, g L^{-1}), y_5 (furfural concentration, g L^{-1}) and y_6 (HMF
680 concentration, %).

	Operational conditions		**Experimental results**					
Exp	**T**	**%**	**Glucose**	**Xylose**	**Arabinose**	**AcH**	**Furfural**	**HMF**
1	-1	-1	0.86	0.37	3.01	0.94	0.02	0.03
2	-1	0	0.76	5.95	3.21	2.80	0.02	0.02
3	-1	1	0.98	9.91	3.50	3.43	0.03	0.04
4	0	-1	0.99	6.06	3.47	2.37	0.04	0.07
5	0	0	2.46	16.90	3.64	4.60	0.09	0.04
6	0	1	2.40	19.06	3.40	4.64	0.28	0.10
7	1	-1	2.72	19.83	4.18	4.35	0.15	0.13
8	1	0	6.69	22.17	3.89	5.08	0.50	0.14
9	1	1	4.33	20.05	3.13	4.73	0.73	0.19
10	0	0	2.14	14.37	3.70	3.94	0.08	0.03
11	0	0	2.37	17.58	3.74	4.47	0.11	0.05
12	0	0	2.39	17.63	3.75	4.32	0.12	0.05

681 AcH: acetic acid; HMF: hydroxymethylfurfural
682
683
684

685 **Table 4.** ANOVA for the second-order polynomial model and coefficients of determination.

y_1 (Glucose)						
Factor	**Sum of squares**	**Degree of freedom**	**Mean square**	**F-value**	***p*-value**	***Significant level***
x_1 (L+Q)	12.74	2	6.37	340.30	0.00	*
x_2 (L+Q)	2.19	2	1.09	58.35	0.00	*
x_1*x_2	0.55	1	0.55	29.59	0.01	**
Lack of Fit	0.43	3	0.14	7.73	0.06	
Pure Error	0.06	3	0.02			
Total SS	15.78	11				
R-sqr = 0.97; Adj: 0.94; MS Pure Error = 0.02						
y_2 (Xylose)						
Factor	**Sum of squares**	**Degree of freedom**	**Mean square**	**F-value**	***p*-value**	***Significant level***
x_1 (L+Q)	354.40	2	177.20	75.19	0.00	*
x_2 (L+Q)	107.06	2	53.53	22.71	0.01	**
x_1*x_2	21.74	1	21.74	9.23	0.05	
Lack of Fit	26.99	3	8.99	3.82	0.15	
Pure Error	7.07	3	2.36			
Total SS	527.62	11				
R-sqr = 0.93; Adj: 0.88; MS Pure Error = 2.36						
y_3 (Arabinose)						
Factor	**Sum of squares**	**Degree of freedom**	**Mean square**	**F-value**	***p*-value**	***Significant level***
x_1 (L+Q)	0.38	2	0.19	77.62	0.00	*
x_2 (L+Q)	0.16	2	0.08	32.23	0.00	*
x_1*x_2	0.59	1	0.59	245.12	0.00	*
Lack of Fit	0.06	3	0.02	8.37	0.06	
Pure Error	0.01	3	0.00			
Total SS	1.23	11				
R-sqr = 0.94; Adj: 0.90; MS Pure Error = 0.02						
y_4 (Acetic acid)						
Factor	**Sum of squares**	**Degree of freedom**	**Mean square**	**F-value**	***p*-value**	***Significant level***
x_1 (L+Q)	8.33	2	4.16	52.26	0.00	*
x_2 (L+Q)	5.73	2	2.86	35.93	0.00	*
x_1*x_2	1.12	1	1.12	14.04	0.03	*
Lack of Fit	0.27	3	0.09	1.15	0.45	
Pure Error	0.24	3	0.08			
Total SS	16.26	11				
R-sqr = 0.97; Adj: 0.94; MS Pure Error = 0.80						
y_5 (Furfural)						
Factor	**Sum of squares**	**Degree of freedom**	**Mean square**	**F-value**	***p*-value**	***Significant level***
x_1 (L+Q)	0.32	2	0.16	664.20	0.00	*
x_2 (L+Q)	0.12	2	0.06	242.22	0.00	*
x_1*x_2	0.08	1	0.08	333.50	0.00	*
Lack of Fit	0.01	3	0.00	9.49	0.05	**
Pure Error	0.00	3	0.00			
Total SS	0.54	11				
R-sqr = 0.98; Adj: 0.97; MS Pure Error = 0.00						
y_6 (HMF)						
Factor	**Sum of squares**	**Degree of freedom**	**Mean square**	**F-value**	***p*-value**	***Significant level***
x_1 (L+Q)	0.02	2	0.01	205.23	0.00	*
x_2 (L+Q)	0.00	2	0.00	34.28	0.01	*
x_1*x_2	0.00	1	0.00	7.96	0.06	**
Lack of Fit	0.00	3	0.00	1.90	0.30	
Pure Error	0.00	3	0.00			
Total SS	0.03	11				
R-sqr = 0.98; Adj: 0.97; MS Pure Error = 0.00						
Significant coefficients at the 99% confidence level (*) or 95% (**)						

686 **Table 5.** Chemical composition of the raw and detoxified hydrolyzates (with 1, 2.5 and 5%
687 (w/v) activated charcoal).

	Raw	1% (w/v)	2.5% (w/v)	5% (w/v)
Sugars and acids				
Glucose	5.15±0.10	4.15±0.01	3.90±0.00	3.53±0.08
Xylose	17.24±0.20	13.78±0.05	13.58±0.09	12.66±0.16
Arabinose	3.47±0.07	2.46±0.03	2.44±0.03	2.37±0.24
Oxalic acid	1.63±0.01	2.40±0.24	2.21±0.13	2.00±0.16
Tartaric acid	1.75±0.02	1.67±0.13	1.62±0.01	1.46±0.02
Aliphatic acids				
Acetic acid	4.16±0.14	4.45±0.09	4.22±0.00	4.13±0.09
Furan derivatives				
Furfural	0.25±0.02	0.04±0.01	n.d.	n.d.
HMF	0.06±0.00	0.05±0.00	0.03±0.00	0.02±0.00
Phenolic compounds				
Phenolic compounds*	2.38±0.00	0.27±0.00	0.10±0.00	0.02±0.00
% color removal	-	51.30±0.28	80.21±1.74	95.27±0.03

688 n.d.: not detected.
689 *expressed as equivalent to gallic acid

690

691

692

693

694

695

696

697

698

699

Table 6. Stoichiometric parameters (g L^{-1}), productivities and yields for bioconversion assays carried out by *L. plantarum*, *L. pentosus* and *L. lactis* grown in raw or detoxified diluted hemicellulosic hydrolyzates.

	L. plantarum		*L. pentsosus*		*L. lactis*	
	RHH	DHH	RHH	DHH	RHH	DHH
Glucose $_{\text{time 0}}$ (g/L)	4.66	4.38	4.86	4.42	4.82	4.33
Glucose $_{\text{time t}}$ (g/L)	4.62	1.47	4.50	2.06	4.98	2.03
Xylose $_{\text{time 0}}$ (g/L)	7.57	6.02	7.66	6.04	7.19	6.04
Xylose $_{\text{time t}}$ (g/L)	7.52	3.64	7.41	3.77	7.00	4.42
Arabinose $_{\text{time 0}}$ (g/L)	1.90	1.65	1.35	1.71	1.86	1.68
Arabinose $_{\text{time t}}$ (g/L)	1.96	0.00	1.97	0.00	2.01	1.32
Lactic acid $_{\text{time 0}}$ (g/L)	0.00	0.67	1.00	0.72	0.95	0.61
Lactic acid $_{\text{time t}}$ (g/L)	0.00	6.85	0.99	6.56	0.88	4.15
Acetic acid $_{\text{time 0}}$ (g/L)	8.75	6.32	6.50	6.35	6.68	6.22
Acetic acid $_{\text{time t}}$ (g/L)	7.08	6.94	6.75	6.79	6.90	5.98
Time (h)	36	12	36	20	36	20
Q_P (g/L·h)	0.00	0.51	0.00	0.29	0.00	0.18
Q_S (g/L·h)	0.00	0.58	0.00	0.32	0.00	0.21
$Y_{P/S}$ (g/g)	0.00	0.89	0.80	0.92	0.66	0.83

RHH: raw hemicellulosic hydrolyzates
DHH: detoxified hemicellulosic hydrolyzates
Time: fermentation times corresponding to the transition from high to low slope of the sigmoidal lactic acid profiles
Q_P, global volumetric productivity of lactic acid
Q_S, sugars (glucose + xylose + arabinose) consumption rate
$Y_{P/S}$, lactic acid yield (g lactic acid produced g^{-1} sugars consumed).

FIGURE LEGENDS

Figure 1. Pareto chart for a) glucose, b) xylose, c) arabinose, d) acetic acid, e) furfural and f) HMF.

Figure 2. Dependence of a) glucose, b) xylose, c) arabinose, d) acetic acid, e) furfural and f) HMF on temperature (coded) and H_2SO_4 concentration (coded).

Figure 3 Profiles for predicted values and desirability model to determine optimum xylose released. Dashed lines indicate the optimization values.

Figure 4. Course with time of color removal using different concentrations of charcoal (w/v): 1% (■), 2.5% (•) and 5% (▲).

Figure 5. Profile of sugars consumption, and the production of lactic acid and acetic acid, by a) *L. plantarum*; b) *L. pentosus*; and c) *L. lactis* grown in raw diluted hemicellulosic hydrolyzates (left column) or diluted hemicellulosic hydrolyzates (right column) detoxified with 5% (w/v) charcoal: Glucose (♦), xylose (•), arabinose (×), lactic acid (■) and acetic acid (▲).

Figure

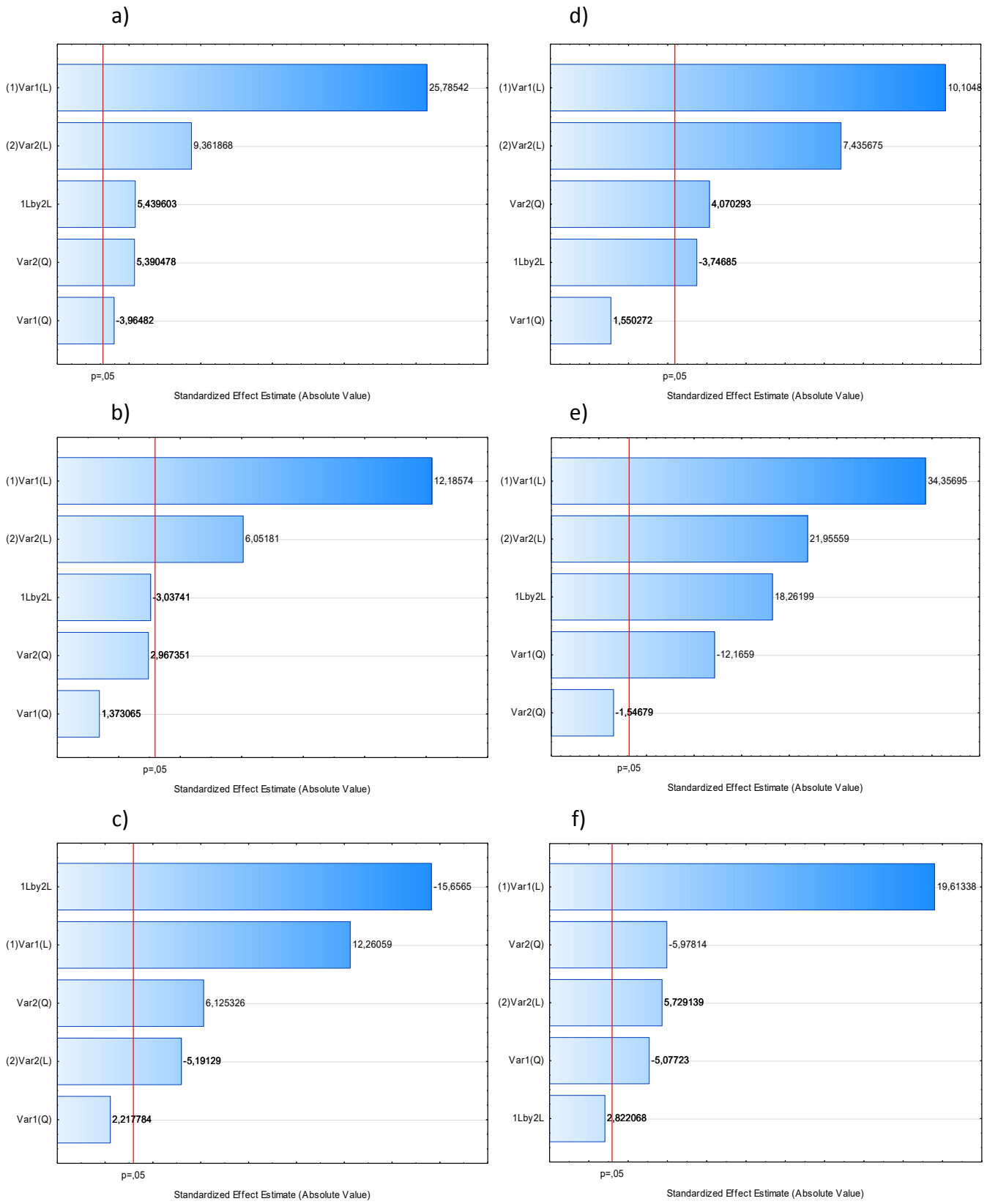

Figure 1

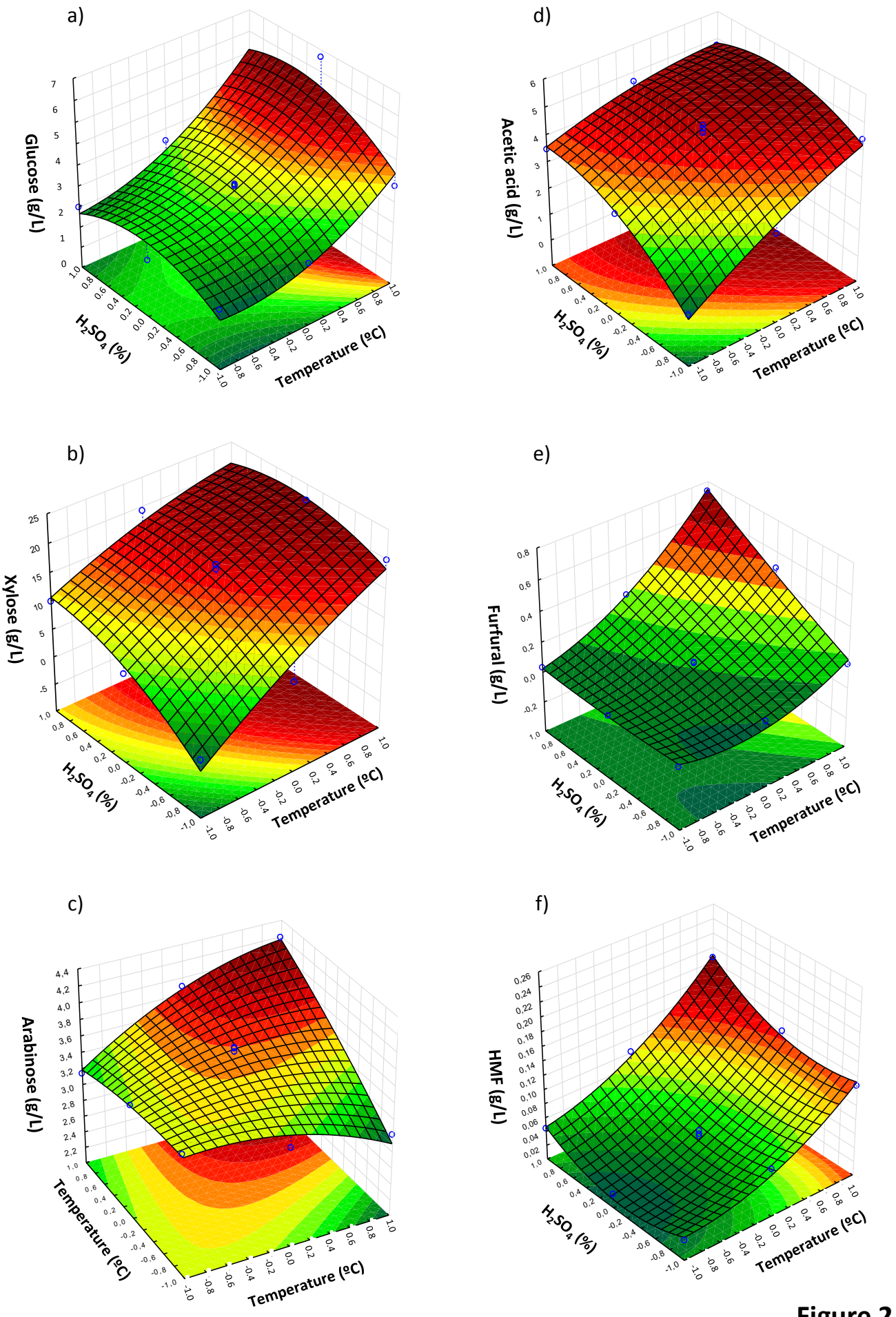
a)
Glucose (g/L)
H_2SO_4 (%)
Temperature (ºC)
b)
Xylose (g/L)
H_2SO_4 (%)
Temperature (ºC)
c)
Arabinose (g/L)
Temperature (ºC)
Temperature (ºC)
d)
Acetic acid (g/L)
H_2SO_4 (%)
Temperature (ºC)
e)
Furfural (g/L)
H_2SO_4 (%)
Temperature (ºC)
f)
HMF (g/L)
H_2SO_4 (%)
Temperature (ºC)

Figure 2

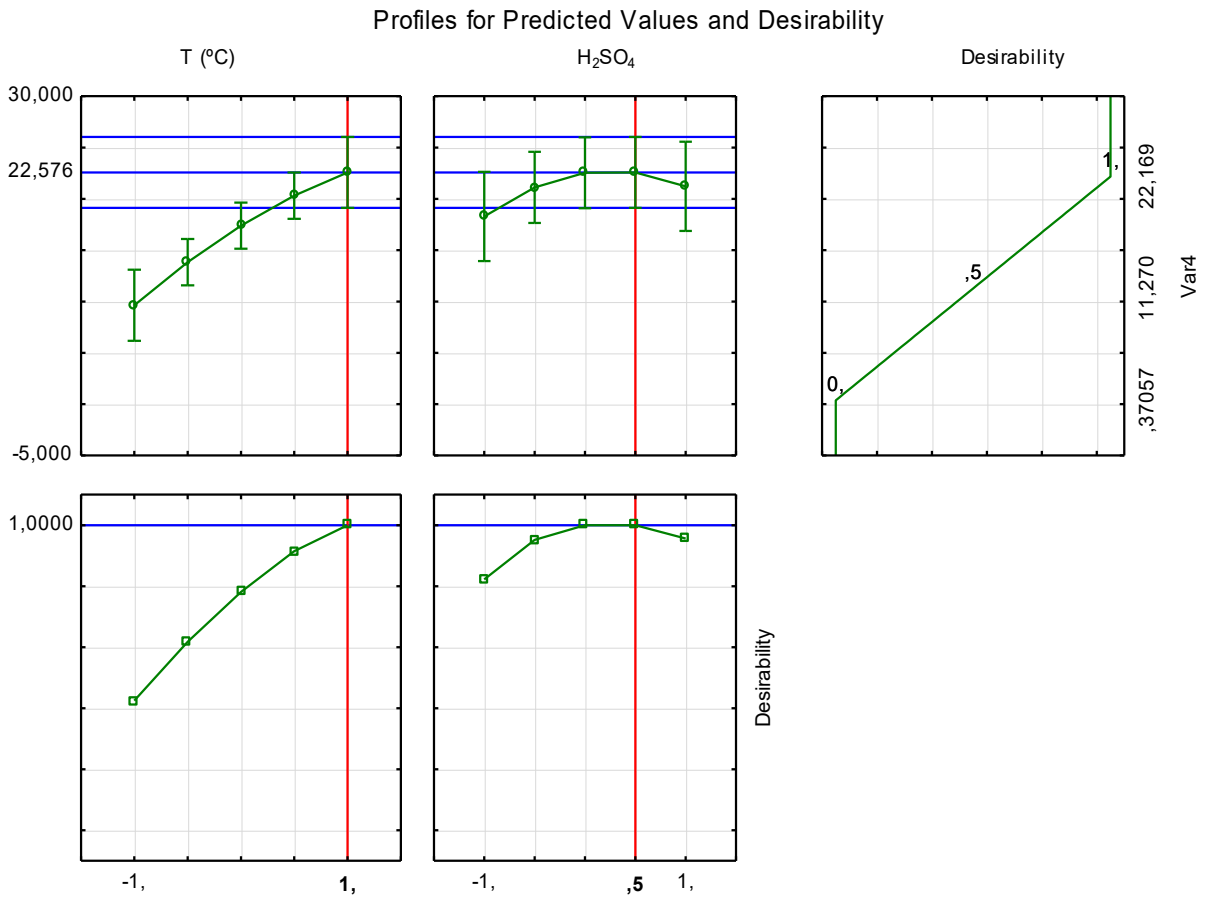
Profiles for Predicted Values and Desirability
T (ºC)
H2SO4
Desirability
30,000
22,576
-5,000
1,0000
-1,
1,
-1,
,5
1,
0,
,5
1,
22,169
11,270
,37057
Var4
Desirability

Figure 3

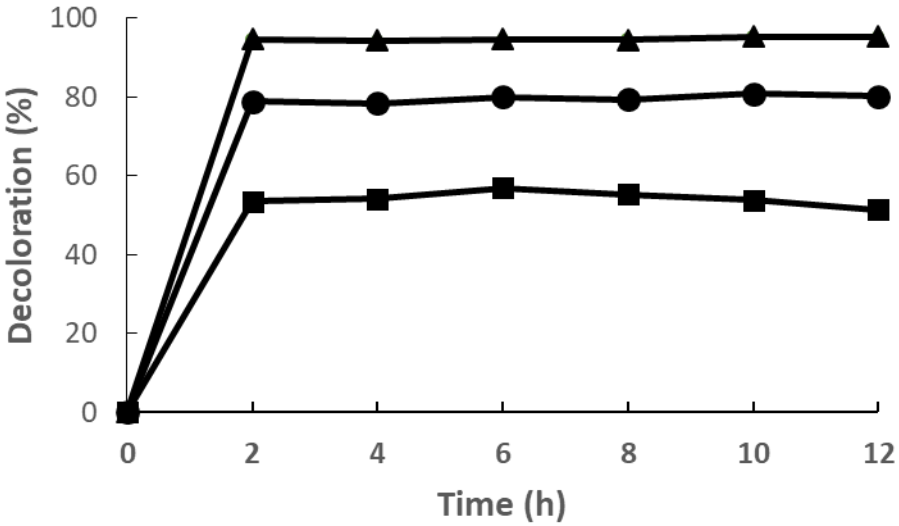

Figure 4

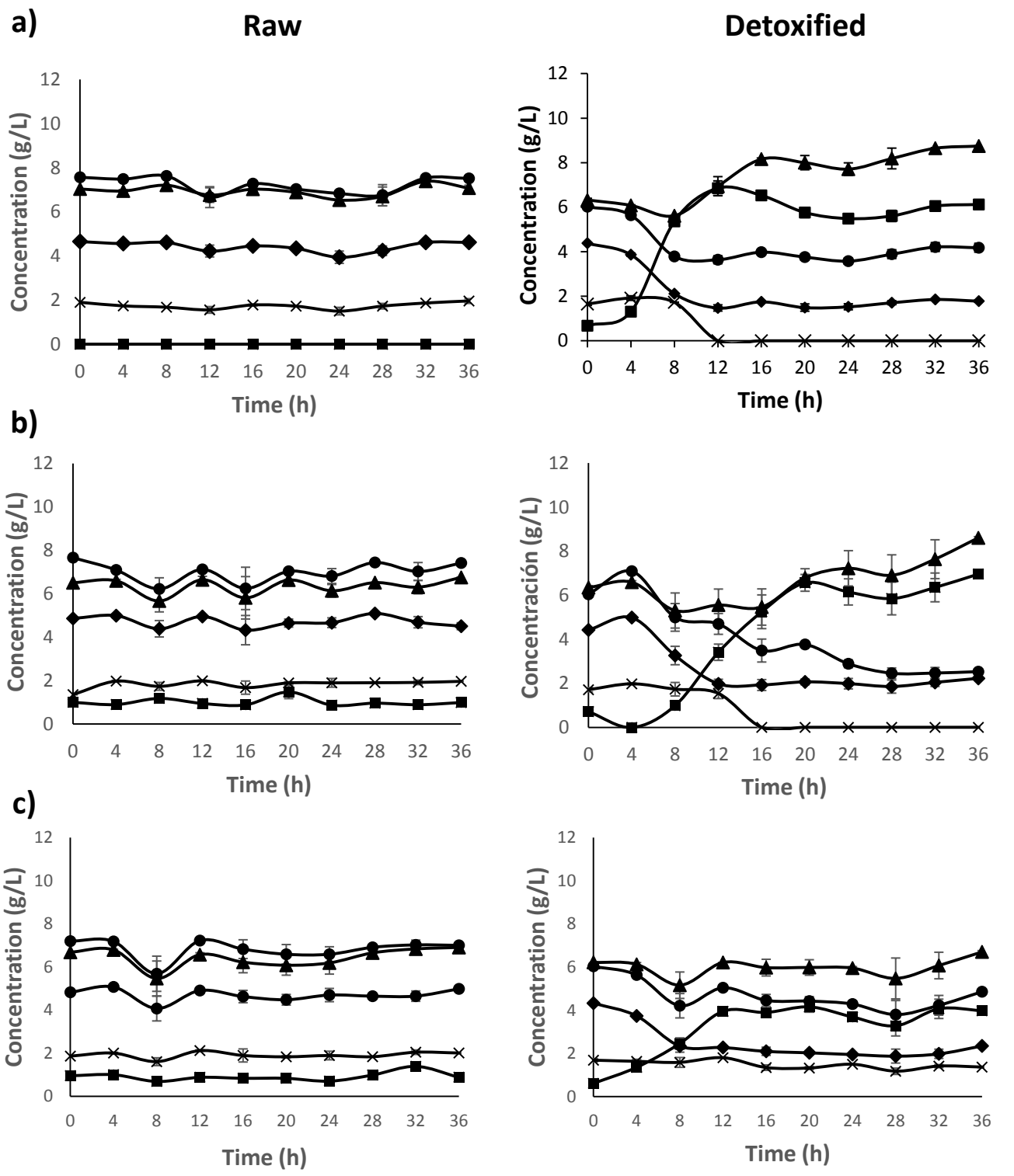
a)
Raw
Detoxified
b)
c)
Concentration (g/L)
Concentración (g/L)
Time (h)
0
2
4
6
8
10
12
0
4
8
12
16
20
24
28
32
36

Figure 5